

# **Θ-STOCK, A POWERFUL TOOL OF THERMOHYDROMECHANICAL BEHAVIOUR AND DAMAGE MODELLING OF UNSATURATED POROUS MEDIA**

**Behrouz Gatmiri,<sup>a,b</sup> Chloe Arson,<sup>a</sup>**

<sup>a</sup> Université de Paris Est, Institut Navier, Ecole Nationale des Ponts et Chaussées, Paris

<sup>b</sup> University of Tehran, Tehran

## **1 ABSTRACT**

A brief review of the basic points of a suction-based heat, moisture transfer and skeleton deformation equations for an unsaturated medium is presented. The main issues such as: two temperature-dependent state surfaces of void ratio and degree of saturation which are used to present the coupling effects of temperature, moisture content and deformation of skeleton; the new thermoelastoplastic constitutive law and etc are briefly mentioned. The Bubnov-Galerkin integral form of field equations has been developed as the basis of spatial and temporal discretized matrix form. The single step integration in time is described. The numerical solution algorithm of the finite element package, **Θ-STOCK**, is presented. Some application cases are presented and discussed to show the strong ability of presented model and the prepared numerical package.

*Keywords:* Unsaturated soil, Thermohydromechanical behaviour, Finite element method, Damage modeling, Elastoplastic behaviour, Multiphase porous media.

## **2 INTRODUCTION**

Since the soil is continuously under the effect of temperature changes in its natural environment, a great deal of attention has been paid to the phenomenon of moisture transport due to thermal gradient from at least the beginning decades of the past century. In the earlier investigations the critical role of unsaturated zone near the soil surface in the groundwater recharge, surface runoff and evapo-transpiration of the precipitation was the center of attention, but in the latter studies major attentions have been focused on geothermal energy extraction, contaminant transport and specially the safe disposal of high-level radioactive waste. The engineered clay barriers are currently used for the filling and sealing of the underground nuclear waste repositories. Considering the unsaturated state of such deformable materials, a

deep understanding of coupling effects of moisture, heat, air and soil deformation seems to be an absolute necessity.

The phase changes between liquid and gas, evaporation, condensation, induced moisture transfer under thermal and pore pressure gradients and the effects of moisture distribution on heat flow are important aspects in non-deformable unsaturated porous media. If the deformation of porous media, which is significant in engineered clay barriers, is considered, the coupling effects among deformation, moisture, and heat should also be addressed in addition of all above aspects.

Philip and de Vries [1] and de Vries [2] theory assumes that the moisture transfer in unsaturated soil occurs in both vapor and liquid phases, under the combined influence of gravity, the gradient of temperature and the gradient of moisture content. This theory makes a consistent distinction between liquid and vapor phases concerning the changes of moisture content.

Another theory for the analysis of coupled mass and heat transfer in porous media was developed by Taylor and Cary [3], who used the general theory of irreversible thermodynamics processes (TIP). Laboratory experiments performed by Cassel et al. [4] showed that this approach underestimated the flow rate by a factor of 10 to 40. It seems this approach did not consider the problem of integration from the microscopic scale to the macroscopic scale rigorously enough. This is a real lack, since the mechanical equations are currently written by means of this integration.

Dirksen [5] studied the soil moisture movement in a freezing column of soil, in absence of water table. He observed a good agreement with Philip and de Vries' theory. The laboratory experiments of Cassel et al. [4] proved to be in a close correlation with the Philip and de Vries' theory.

The theory of Philip and de Vries is now generally accepted in soil sciences and geotechnical engineering studies. However, this theory encompasses some restrictions in geotechnical engineering practice, which should be overcome. One of these limitations lies in the assumption of incompressibility of the soil skeleton. It is not realistic, especially in the case of engineered clay barriers, which are soft and significantly deformable. The  $\theta$ -based formulation, which was initially chosen by Philip and de Vries for the presentation of their theory, is valid for homogeneous soils and cannot take hysteretic effects into account. In order to overcome these latter restrictions, two attempts have been reported by Sophocleous

[6] and Milly [7]. Both of these works have been undertaken with the aim of converting the  $\theta$ -based formulation of Philip and de Vries to a matric head-based formulation in order to consider soil inhomogeneity and hysteretic effects in desiccation and resaturation conditions.

Sophocleous [6] has begun with Philip and de Vries [1] model and does not consider hysteresis, while Milly [7] considers de Vries [2] model which in a more general frame. Milly [7] has criticized Sophocleous' [6] work and has found apparently two major errors.

Thomas [8] has presented a simple numerical solution of the  $\theta$ -based formulation of Philip and de Vries, ignoring the convection effects in an incompressible soil. Thomas and He [9] have presented the moisture and heat transfer analysis in a deformable unsaturated soil.

Geraminegad and Saxena [10] may have been the first investigators who have developed a model in which the soil deformation is considered. Their model does not include soil deformations due to external loading. In this formulation, soil deformation was limited to volumetric deformation due to pore air pressure and suction change.

Coleman [11] and Bishop and Blight [12] have found out the basic frame of two stress state variables approaches. Fredlund and Morgenstern [13,14] have shown that any pair of three stress parameters  $\sigma$ - $P_a$ ,  $\sigma$ - $P_w$ ,  $P_a$ - $P_w$  would be sufficient to describe the mechanical behavior of unsaturated soils. For the last three decades, net stress  $\sigma$ - $P_a$ , and matrix suction  $P_a$ - $P_w$  have been the most commonly used variables. Various constitutive laws have been used, such as the incremental elastic formulation suggested by Coleman [11] and Fredlund [14], and the state surface concept developed in order to describe the volumetric behavior of soil under the coupled effects of net stress and suction changes. Matyas and Radhakrishna [16] have compared experimental data to the predictions given by the state surfaces of the void ratio and the degree of saturation. Fredlund [15] has proposed explicit mathematical expressions for both state surfaces. Lloret and Alonso [17] have given alternative expressions. Gatzmire [18] has developed an explicit expression of the void ratio state surface, which is compatible with nonlinear elastic (hyperbolic) constitutive laws (Gatzmire [18], Gatzmire and Delage [19]).

Starting from the approach proposed by Alonso et al [20], which is an elastic model, a nonlinear elastic model of unsaturated soil has been developed at the CERMES since 1989. A new state surface formulation has been performed. This model has been incorporated within U-DAM finite element code, developed by the two mentioned authors to model the behaviour and transfer laws characterizing an unsaturated soil (Nanda [21], Gatmiri [22,23]), Gatmiri et al. [24]). The important aspects of earthdam construction are considered in this code.

Another finite element code with elastoplastic constitutive law has also been developed by Gatmiri et al [25]. Nonlinear elastic models have the advantage to be easily numerically implemented. Moreover, the involved material parameters are easy to determine and to measure. Considering the hysteretic phenomenon due to desiccation and wetting cycles by a unique state surface, is a restriction. Though, this difficulty can be overcome by using two different formulations of volumetric changes, corresponding to two paths of moisture changes in desiccation and wetting.

The theory of Philip and de Vries [1] and de Vries [2] is a comprehensive theory of moisture and heat movement in an incompressible porous medium. It found the new suction-based mathematical model presented by Gatmiri [26], Gatmiri et al [27,28] and Gatmiri ([29,30]. to study the thermo-hydro-mechanical behavior of unsaturated media. In this approach, heat and moisture transfer equations are given in an alternative form, based on water and air pressures. This model has been formulated with the two most widely used independent state variables: net stress and suction. It describes the water and air pore pressures distribution, and the deformation of the skeleton. The coupling effects of temperature and moisture content on the deformation of the skeleton, and their inverse effects, are included in the model, via thermal a state surface concept. Temperature-dependent state surface formulations are given for the void ratio and degree of saturation variations within the porous media. A non-linear constitutive strain-stress relationship is considered. In this new type of formulation, the soil non-homogeneity, as well as hysteretic effects, may be included. The phase change between liquid and vapor phases is taken into account.

A mixed damage model, formulated in net stress and suction, has also been developed in order to represent fracturing around Excavation Damaged Zones. Behaviour laws are derived from a thermodynamic potential, which encompasses localization-regularization terms. Damage rigidities associated to the state



variables are computed by applying the Principle of Equivalent Elastic Energy, which is widely used in micromechanics. Homogenized cracking parameters are also included in the expression of the intrinsic liquid permeability of the medium, in order to represent the influence of damage on fluid transfers. Because of the complexity of the established governing partial differential equations, a numerical resolution scheme has been developed, by means of the finite element method. Bubnov - Galerkin integral forms of field equations are taken into consideration as the basis for the spatial and temporal discretized matrix form of the equilibrium equations. Only one integration step is used in time. (θ - STOCK) code has been validated by several applications. For the sake of brevity of the text the literature review has been omitted. An exhaustive literature review has been given in Gatmiri [29,30].

### **3 THE PROPOSED MODEL**

In this model, two basic theories are modified and combined in order to describe a fully coupled behavior of unsaturated porous medium under heating. In the one hand, the nonlinear theory of isothermal behavior of unsaturated soil under the coupled effects of net stress and suction is extended to isothermal conditions. The reasoning is founded on the concept of state surfaces for the void ratio and the degree of saturation, exposed in the previous works of Gatmiri [19,20,31]. In the other hand, Philip and de Vries' theory of heat and moisture transfer is modified in order to take the deformation of the skeleton into account. This fully coupled formulation is presented in a new, suction-based formulation, which is more suitable for a combination with the deformation theory of unsaturated soils.

#### ***3.1 Moisture phase equations***

Moisture is composed of vapor and liquid phases. As already mentioned and by Philip and de Vries [1], the term 'liquid transfer' is used for the transfer, which occurs exclusively in liquid phase. Excess transfers, coming in addition to liquid transfers are called 'vapour transfer'.

The total moisture movement in an unsaturated soil submitted to a temperature gradient and its resulting moisture content gradient, is the superposition of the flows that take place separately in each phase (vapour and liquid). Hence, the total moisture transfer governing equation, defined as the sum of liquid and vapour velocities, can be written as follows:

$$\frac{q}{\rho_w} = -D_T \nabla T - D_\theta \nabla \theta - D_w \nabla Z \quad (1)$$

Where  $D_T$  is the thermal moisture diffusivity, which is equal to the sum of the thermal vapour and water diffusivities.  $D_\theta$  is the isothermal moisture diffusivity, which is equal to the sum of the isothermal vapour and water diffusivities.  $D_w \nabla Z$  ( $D_w = K_w = K_{wz0} [(S_r - S_{r0}) / (1 - S_{r0})]^b (v_r / v_T)$  (where  $v$  is the dynamic viscosity of water and  $K_{wz0}$  is the saturated soil water permeability)) is the gravitational part of the equation. More details about these parameters can be found in Gatmiri [26] and Gatmiri et al. [32-36]. Concerning the moisture mass conservation equation, the same concept is used. Hence, the following form is proposed:

$$\frac{\partial(\theta \rho_w + (n - \theta) \rho_v)}{\partial t} = \frac{\partial(n S_r \rho_w + n(1 - S_r) \rho_v)}{\partial t} = -\text{div}(\rho_w (U + V)) \quad (2)$$

$V$  is the vapour velocity,  $U$  is the water velocity,  $\theta$  is the volumetric water content,  $n$  is the porosity,  $S_r$  is the degree of saturation in water and  $\rho_w$  and  $\rho_v$  are, respectively, the water and the water vapour densities.

The introduction of thermal state surfaces of the degree of saturation and the void ratio is a new important point of the theory developed by Gatmiri [3]. These surfaces are described in the following sections. The thermal state surface of the degree of saturation relates the variation of the degree of saturation to the state of suction, temperature and net stress in the soil. The idea of Water Retention Curve, which considers only the effect of suction on the variation of water content, is extended via the thermal state surface to the temperature and net stress variations occurring in the soil. By combining the equations (1) and (2), the final partial differential equation for the moisture in an unsaturated soil can be written as the following:

$$\begin{aligned} & n S_r \left( \frac{\partial \rho_w}{\partial T} \right)_{P_w = cte} \frac{\partial T}{\partial t} + n S_r \left( \frac{\partial \rho_w}{\partial P_w} \right)_{T = cte} \frac{\partial p_w}{\partial t} + (\rho_w - \rho_v) n \frac{\partial S_r}{\partial t} + \\ & (S_r \rho_w + \rho_v (1 - S_r)) \frac{\partial n}{\partial t} + n(1 - S_r) \frac{\partial \rho_v}{\partial t} = \\ & \text{div}(\rho_w D_w \nabla Z) + \text{div}(\rho_w D_T \nabla T) + \text{div}(\rho_w D_p \nabla (P_w - P_g)) \end{aligned} \quad (3)$$

### 3.2 Gas phase equations

Considering the generalized Darcy's law for the motion of gas in the soil, the gas flow equation is:

$$V_g = \frac{q_g}{\rho_g} = \frac{-K_g}{\gamma_g} \frac{\partial P_g}{\partial T} \nabla T - K_g \left( \nabla \left( \frac{P_g}{\gamma_g} \right) + \nabla Z \right) \quad (4)$$

where  $V_g$  is the vector of velocity,  $q_g$  is the vector of flow,  $\rho_g$  is the mass density,  $K_g = (b\gamma_g/\mu_g)[e(1-S_r)]^c$  is the air permeability,  $P_g$  is the gas pressure and  $\gamma_g$  is the specific weight of the gas. In these equations, it is assumed that gas pore pressure depends on temperature.

The governing differential equation for the mass conservation of the gas phase may be expressed in controlled volume of unsaturated porous medium, as follows:

$$\frac{\partial}{\partial t} [n\rho_g (1 - S_r + HS_r)] = -\text{div}(\rho_g V_g) - \text{div}(\rho_g HU) + \rho_w \text{div} V \quad (5)$$

where  $H$  is Henry's constant, which corresponds to the dissolution of air in water. The first term of the right hand side of this equation is related to gas flow due to gas pressure gradient, the second term denotes the motion of dissolved air in water, while the gas loss by vapour condensation is represented by the third term. Hence, the general partial differential equation of gas movement for unsaturated cases in suction-based formulation may be deduced from equations (4) and (5):

$$\begin{aligned} \rho_g (1 - S_r (1 - H)) \frac{\partial n}{\partial t} + n(1 - S_r (1 - H)) \frac{\partial \rho_g}{\partial t} - (1 - H) n \rho_g \frac{\partial S_r}{\partial t} = \\ \text{div} \left[ \left( \rho_g K_g \frac{\partial P_g}{\gamma_g \partial T} + H \rho_g D_{Tw} - \rho_w D_{TV} \right) \nabla T \right] + \\ \text{div} \left[ \left( \frac{K_g \rho_g}{H \rho_g D_{Pw} - \rho_w D_{Pv}} - H \rho_g D_{Pw} + \rho_w D_{Pv} \right) \nabla P_g \right] + \text{div} \left[ \left( \frac{K_g \rho_g}{H \rho_g D_{Pw} - \rho_w D_{Pv}} + H \rho_g D_{Pw} \right) \nabla Z \right] \end{aligned} \quad (6)$$

### 3.3 Solid skeleton behavior

Considering the two stress state variables as suction and net stress, the equilibrium equation and the constitutive law of a non-isothermal, isotropic and non-linear medium may be based on isothermal equations, as follows:

- *Equilibrium equation:*

$$(\sigma_{ij} - \delta_{ij} p_g)_{,j} + p_{g,i} + b_i = 0 \quad (7)$$

Under the assumption of small deformations, the constitutive law for the solid skeleton of a saturated soil, which is under suction and thermal effects can be written as:

$$F = DD_s^{-1} \text{ with } D_s^{-1} = \beta_s m, \text{ in which } \beta_s = \frac{1}{1 + e} \frac{\partial e}{\partial (P_g - P_w)},$$

$$\text{-----} \quad \text{with } D_t^{-1} = \beta_t m, \text{ in which } \beta_t = \frac{1}{1 + e} \frac{\partial e}{\partial (T)} \text{ and } m = [1 \ 1 \ 0]. \quad (9)$$

In order to calculate the bulk modulus, the volumetric strain can be taken into account via a void ratio state surface, which depends on stress, suction and temperature. Using the same approach as in Gatmiri [19], Gatmiri and Delage [20] and Gatmiri et al [24], a new formulation of the void ratio state hyper surface is proposed, as the following:

Although the stress-strain behavior is already coupled with temperature, the description of the coupling of volumetric moisture content with temperature is also necessary to model an unsaturated soil submitted to stress and suction. Based on experimental data, the following state surface of degree of saturation is proposed:

where  $a_s$ ,  $b_s$ ,  $c_s$  and  $d_s$  are constant. A schematic presentation of this surface is given in Fig. 5.

### 3.4 Heat equations

Following Philip and de Vries theory, the total flow of latent and sensible heat in an unsaturated porous medium can be given by:

$$Q = -\lambda \text{grad}T + \rho_w h_{fg} V + \rho_v V h_{fg} + [C_{pw} \rho_w U + C_{pv} \rho_w V + C_{pg} \rho_g V] (T - T_0) \quad (12)$$

where  $C_{pw}$ ,  $C_{pv}$  and  $C_{pg}$  are the water, vapour and gas heat capacities,  $T_0$  is an arbitrary reference temperature,  $h_{fg}$  is the latent heat of vaporisation and  $\lambda$  is Fourier heat diffusion coefficient. It can be evaluated by the following proposed equation:

$$\lambda = (1 - n)\lambda_s + \theta\lambda_w + (n - \theta)\lambda_v \quad (13)$$

$\lambda_s$ ,  $\lambda_w$  and  $\lambda_v$  denote respectively, soil, water and vapour heat diffusion coefficients.

In eqn (12), the first term is related to conductive heat flow, the next two terms represent the evaporation phenomenon and the latter one denotes the convective heat flow in liquid, vapour and gas phases. The importance of the terms related to the evaporation of water will be investigated in the treated numerical example.

The energy conservation equation in a porous medium can be expressed by:

$$\frac{\partial \varphi}{\partial t} + \text{div}Q = 0 \quad (14)$$

where  $Q$  is the heat flow and  $\varphi$  is the volumetric bulk heat content of medium, which can be defined by:

$$\varphi = C_T (T - T_0) + (n - \theta)\rho_v h_{fg} \quad (15)$$

$C_T$  is the specific heat capacity of the unsaturated mixture and can be written as:

$$C_T = (1 - n)\rho_s C_{ps} + \theta\rho_w C_{pw} + (n - \theta)\rho_v C_{pv} + (n - \theta)\rho_g C_{pg} \quad (16)$$

The final differential form of the heat flow equation in unsaturated porous media is found by combining equations (13-16):

$$C_T \frac{\partial T}{\partial t} + (T - T_0) \frac{\partial C_T}{\partial t} + (1 - S_r)\rho_v h_{fg} \frac{\partial n}{\partial t} - n\rho_v h_{fg} \frac{\partial S_r}{\partial t} + n(1 - S_r)h_{fg} \frac{\partial \rho_v}{\partial t} - \text{div}[\lambda(\theta) \nabla T] +$$

$$\frac{C_{pw}\rho_w}{C_{pv}\rho_w} \text{div} \left[ \left( -D_{Tv} \nabla T - D_{Pv} \nabla \left( \frac{P_w}{P_g} - \frac{P_g}{P_g} \right) \right) (T - T_0) \right] +$$

$$\begin{aligned}
& C_{pg} \operatorname{div} \left[ -\frac{\rho_g K_g}{\gamma_g} \frac{\partial P_g}{\partial T} \nabla T - \rho_g K_g \left( \frac{\nabla \rho_g}{\gamma_g} + \nabla Z \right) \right] (T - T_0) + \\
& h_{fg} \operatorname{div} \left[ -\frac{\rho_v K_g}{\gamma_g} \frac{\partial P_g}{\partial T} \nabla T - \rho_v K_g \left( \frac{\nabla \rho_g}{\gamma_g} + \nabla Z \right) \right] + \\
& \rho_w h_{fg} \operatorname{div} [-D_{Tv} \nabla T - D_{Pv} \nabla (P_w - P_g)] = 0.
\end{aligned} \tag{17}$$

The general initial and boundary conditions should be associated with the preceding equations to complete the mixed initial boundary value problem of thermohydromechanics for unsaturated soils. These conditions are given in the following section.

#### 4 GENERAL INITIAL AND BOUNDARY CONDITIONS:

$$u(x, 0) = 0 \quad \text{on } \Omega \tag{18}$$

$$p_w(x, 0) = p_{w0} \quad \text{on } \Omega \tag{19}$$

$$p_g(x, 0) = p_{g0} \quad \text{on } \Omega \tag{20}$$

$$T(x, 0) = T_0 \quad \text{on } \Omega \tag{21}$$

$$\text{I} \quad \begin{cases} \left\{ u(x, t) = \bar{u}(x, t) \right. & \text{on } S_1 x[0, \infty) \\ \left. \left\{ \sigma(x, t) \cdot \underline{n} = \bar{\sigma}(x, t) \right. \right. & \text{on } S_2 x[0, \infty) \end{cases} \tag{22}$$

$$\text{II} \quad \begin{cases} \left\{ p_w(x, t) = \bar{p}_w(x, t) \right. & \text{on } S'_{w1} x[0, \infty) \\ \left. \left\{ V_w \cdot \underline{n} = q_w(x, t) \right. \right. & \text{on } S'_{w2} x[0, \infty) \end{cases} \tag{23}$$

$$\text{III} \quad \begin{cases} \left\{ p_g(x, t) = \bar{p}_g(x, t) \right. & \text{on } S'_{g1} x[0, \infty) \\ \left. \left\{ V_g \cdot \underline{n} = q_g(x, t) \right. \right. & \text{on } S'_{g2} x[0, \infty) \end{cases} \tag{24}$$

$$\text{IV} \quad \begin{cases} \left\{ T(x, t) = \bar{T}(x, t) \right. & \text{on } S''_1 x[0, \infty) \\ \left. \left\{ \rho_w C_w V_w^1 T \cdot \underline{n} - h_i \cdot \underline{n} = q_t(x, t) \right. \right. & \text{on } S''_2 x[0, \infty) \end{cases} \tag{25}$$

$\Omega$  represents the considered domain and  $S, S', S''$  represent the different parts of the boundary of domain on which the displacement or stress, air or water pressure or their flow, and temperature or heat flow are given. The initial conditions for the different variables ( $u, p_w, p_g, T$ ) must be introduced. In geotechnical applications, the initial displacements are seldom introduced however.

## 5 SOLUTION APPROACH AND FINITE ELEMENT DISCRETIZATION

Regarding to the complexity of the governing partial differential equations of the proposed model, the development of analytical solutions seems to be very difficult, even for simple configurations. It is probably impossible for real boundary and initial conditions. The known numerical approaches such as finite difference, finite element or boundary element methods can be easily used to find the solutions to the proposed formulation, with general boundary and initial conditions. The Bubnov-Galerkin integral forms of field equations have been used as the basis of the spatial and temporal discretized matrix form.

### 5.1 Spatial Discretization

The weighed residual method has been applied, and the weighed functions of Galerkin have ben used to discretize the total spatial domain  $\Omega$ . The global matrix form of the equations, represented in terms of nodal point values of the field variables, is the following::

$$\begin{bmatrix} 0 & 0 & 0 & 0 \\ 0 & -[K_{TT}] & -[K_{Tw}] & -[K_{Tg}] \\ 0 & -[K_{wT}] & -[K_{ww}] & 0 \\ 0 & -[K_{gT}] & -[K_{gw}] & -[K_{gg}] \end{bmatrix} \begin{Bmatrix} U \\ T \\ P_w \\ P_g \end{Bmatrix} + \begin{bmatrix} [R] & [C_T] & [C_w] & [C_g] \\ [C_{TU}] & [C_{Tw}] & [C_{Tg}] & [C_{TT}] \\ [C_{wu}] & [C_{wT}] & [C_{ww}] & [C_{wg}] \\ [C_{gu}] & [C_{gT}] & [C_{gw}] & [C_{gg}] \end{bmatrix} \begin{Bmatrix} \dot{U} \\ \dot{T} \\ \dot{P}_w \\ \dot{P}_g \end{Bmatrix} = \begin{Bmatrix} \dot{F}_\sigma \\ F_T \\ F_w \\ F_g \end{Bmatrix} \quad (26)$$

### 5.2 - Integration in time

In order to discretize in time domain, the single-step integration, defined in the following, is used:

$$\int_{t_0}^{t_1} u(t)dt = [(1 - \beta)u_0 + \beta u_1] \Delta t = [u_0 + \beta \Delta u] \Delta t \quad (27)$$

$$\int_{t_0}^{t_1} \dot{u}(t)dt = \Delta u \quad (28)$$

in which  $u_0$  and  $u_1$  are the values of the variable  $u$  at times  $t_0$  and  $t_1$ . The time step is  $\Delta t = t_1 - t_0$ , and  $\beta$  indicates the type of interpolation,  $\beta = 0$  forward interpolation (fully explicit),  $\beta = 1/2$  linear interpolation (Crank-Nicolson) and,  $\beta = 1$  backwards interpolation (fully implicit).

The final matrix form can be found as:

(29)

$$\begin{Bmatrix} \Delta F_r \\ \beta \Delta t \Delta F_T \\ \beta \Delta t \Delta F_w \\ -\beta \Delta t \Delta F_g \end{Bmatrix} + \Delta t \begin{Bmatrix} F_{T0} - [K_{TT}]T_0 - [K_{Tw}]P_{w0} - [K_{Tg}]P_{g0} \\ F_{w0} - [K_{wT}]T_0 - [K_{ww}]P_{w0} \\ F_{g0} - [K_{gT}]T_0 - [K_{gw}]P_{w0} - [K_{gg}]P_{g0} \end{Bmatrix}$$

The matrices are given in Appendix 2.

## 6 STABILITY AND ACCURACY

The required conditions of stability and accuracy of the solution algorithm of the fully coupled unsaturated equations are described in detail by Gatmiri et al [24 ] and Gatmiri and Magnin [37]. For the isoparametric quadrilateral elements which are used in  $\theta$  - STOCK, the accuracy criteria have been derived for an internal node inside elements as follows:

- The lower limit criteria related to water flow are:

$$\Delta t \geq \frac{\alpha_3 n^2 (\Delta h)^2}{6\theta C_w (n^2 + 1)}, \Delta t \geq \frac{\alpha_3 n^2 (\Delta h)^2}{3\theta C_w (2n^2 - 1)}, \Delta t \geq \frac{\alpha_3 n^2 (\Delta h)^2}{3\theta C_w (2 - n^2)} \quad (30)$$

- The criteria related to air flow are:

$$\Delta t \geq \frac{\beta_2 n^2 (\Delta h)^2}{6\theta C_a (n^2 + 1)}, \Delta t \geq \frac{\beta_2 n^2 (\Delta h)^2}{3\theta C_a (2n^2 - 1)}, \Delta t \geq \frac{\beta_2 n^2 (\Delta h)^2}{3\theta C_a (2 - n^2)} \quad (31)$$

with

$$\begin{array}{cc} \hline & \hline \\ \hline & \hline \end{array}$$

(32)



It should be emphasize that the large value of the above mentioned lower limits can be chosen as a condition to avoid spatial oscillation. As it can be seen, these criteria depend on the variation of both degree of saturation and void ratio state surfaces, as well as on their derivatives.

## 7 $\theta$ - STOCK ALGORITHM

**$\theta$  - STOCK** software is a powerful computational tool designed for the analysis of the thermohydro-mechanical behavior of multiphase media. Many real engineering applications, such as nuclear waste disposal, stability of slopes and landslides under the effect of climatic changes, modelling of the geo environmental aspects (such as transpiration due to trees and evaporation due to soil-atmosphere interaction), can be treated with this software, in an efficient and accurate manner. The main features of  **$\theta$  - STOCK** system are managed directly by Markaz module as shown in Fig. 1. This program has five main parts, each part including many subroutines as described in the following:

- Part I General input data acquisition and initial state computations (stress and suction)
- Part II Nodal force vector generation and data acquisition in time steps
- Part III General stiffness matrix generation and Boundary condition application
- Part IV System solution of final equations
- Part V Post processing of results and secondary computations

Three independent modules(dry, saturated and unsaturated elements) are integrated in  **$\theta$ -STOCK**. Each module can operate independently and together with the other modules.

Fig. 2 and 3 display a more detailed description of the Stiff block, which is the core of the third part. Notice that elementary stiffness matrices are computed with different procedures called Stif4D (dry elements), Stif4C (saturated elements) and Stif4U (unsaturated elements) in a plain strain configuration. A suffix AXI is added to the names of the subroutines for the axisymmetric case.

## 8 CONSTITUTIVE MODELS IN $\theta$ - STOCK

In the actual version of this package, three constitutive models are incorporated for both saturated and unsaturated soils:

Saturated soil:

- -linear thermoelastic,
- -fully coupled non-linear thermoelastic model via « thermal void ratio state surface » concept,
- -thermoelastoplastic model based on critical state theory as it is described in Gatmiri [29] and Gatmiri et al [25].

Unsaturated soil:

- -linear elastic model considering net stress, suction and temperature as state variables.
- -new non-linear elastic model presented by Gatmiri [26,27,29].
- Thermoelastoplastic model based on extension of BBM to thermal effects Gatmiri [29] and Jenab[38]

This program is conceived with this idea that it would be able to analyze the response of a soil in different states of humidity (dry, unsaturated and saturated), under the influence of mechanical and thermal loadings. Thus, three types of elements (dry, saturated and unsaturated elements) are defined in the program. The program has been divided into three distinct blocks, which can work separately or jointly. At the present stage of the work, the program can be used for the modelling of drained, saturated and unsaturated linear and non-linear elastic materials., The development of the elastoplastic behaviour is complete only for the saturated block in this package. Because of the above mentioned development possibilities, , the validation tests have been reported for the elastic behaviour of dry and saturated blocks (Gatmiri [29, 39], Gatmiri and Delage [31]). Some applications have also been presented, as illustrative examples The validation tests compare the results provide by **Θ-Stock** to the analytical solution of a transient heat flow in a dry column of soil, and give code-to-code comparisons for the study of thermoelastic consolidation. Some application cases for the elastoplastic behaviour are presented (Gatmiri [29] and Jenab [38]. In the following section, the thermoelastoplastic constitutive law is briefly described.

### ***8.1 Thermoelastoplastic Constitutive law***

In this model the following main effects of temperature are considered.

- Shrinkage of the elastic domain due to temperature increase,
- dependence of the yield surface and plastic modulus on temperature, and finally

-unviscose plastic flow .

Two new plastic variables will appear, these two variables are not directly observable, therefore they will be classified among the internal variables. The first variable is plastic deformation tensor  $\underline{\underline{\varepsilon_p}}$  and the second is plastic porosity  $n^p$ , but for a plastically incompressible material such as soil:  $\underline{\underline{tr\varepsilon_p}} = n^p$ , thus only one plastic internal variable remains.

The basic elements of thermoplasticity for unsaturated soil are discussed in following order:

- *-yield surface*

In a classical plasticity theory, it is quite generally postulated that yielding can occur only if the stresses  $\sigma$  satisfy the yield criterion

$$F(\sigma, \varepsilon_p, \kappa) = 0 \quad (33)$$

where  $\kappa$  is a strain hardening parameter and  $\varepsilon_p$  is the accumulated plastic strain.

The Basic elastoplastic Barcelona Model (BBM) is extended to the non-isothermal case by considering that the variation of the yield locus under temperature effects is properly represented by the change in maximum isotropic preconsolidation stress  $p_c$ , which is a function of suction, temperature and accumulated thermoplastic strain (Fig. 4) :

$$p_c = p_{c0} \left( 1 + \frac{\alpha}{1 + \exp(-\beta T)} \right) \left( 1 + \frac{\gamma}{1 + \exp(-\delta \varepsilon_p)} \right) \quad (34)$$

with:

$$\begin{aligned} p_{c0} &= p_c(T=0, \varepsilon_p=0) \\ \alpha &= \frac{p_c(T_{max}) - p_{c0}}{p_{c0}} \\ \beta &= \frac{1}{T_{max} - T_0} \ln \left( \frac{1 + \frac{\alpha}{1 + \exp(-\beta T_{max})}}{1 + \frac{\alpha}{1 + \exp(-\beta T_0)}} \right) \\ \gamma &= \frac{p_c(T=0, \varepsilon_{pmax}) - p_{c0}}{p_{c0}} \\ \delta &= \frac{1}{\varepsilon_{pmax}} \ln \left( \frac{1 + \frac{\gamma}{1 + \exp(-\delta \varepsilon_{pmax})}}{1 + \frac{\gamma}{1 + \exp(-\delta \varepsilon_p)}} \right) \end{aligned}$$

- *Flow rule:*

For an associated flow rule, if  $d\varepsilon_p$  denotes the increment of plastic strain during the plastic deformation, , one can obtain (normality rule=associated flow rule ?):

$$\sigma = \frac{E}{1 + \nu} \epsilon + \frac{E\nu}{1 - 2\nu} \epsilon_v \quad (35)$$

in which  $\frac{E\nu}{1 - 2\nu}$  is a proportionality constant.

During an infinitesimal increment of stress, plastic straining may occur, and total strain changes can be given by:

$$d\epsilon = d\epsilon^e + d\epsilon^p \quad (36)$$

In the present model, the thermoelastic strain is related to net stress, suction increment and temperature change by the convenient matrices. Omitting the presentation of mathematical manipulation, the plastic strain can be defined as:

$$d\epsilon^p = \frac{1}{G} \left( \frac{1}{2} \frac{d\sigma}{\sigma} + \frac{1}{2} \frac{d\tau}{\tau} \right) \quad (37)$$

Finding the plastic multiplier and introducing it into the equation (35), the stress- strain relationship in its final general form can be obtained:

$$\sigma = \frac{E}{1 + \nu} \epsilon + \frac{E\nu}{1 - 2\nu} \epsilon_v + \frac{E\nu}{1 - 2\nu} \frac{1}{G} \left( \frac{1}{2} \frac{d\sigma}{\sigma} + \frac{1}{2} \frac{d\tau}{\tau} \right) \quad (38)$$

with:

$$\frac{1}{G} = \frac{1}{2} \left( \frac{1}{\mu} + \frac{1}{\lambda} \right)$$

and

$$\frac{1}{\mu} = \frac{1}{G} \left( \frac{1}{2} \frac{d\sigma}{\sigma} + \frac{1}{2} \frac{d\tau}{\tau} \right)$$

$$\frac{1}{\lambda} = \frac{1}{G} \left( \frac{1}{2} \frac{d\sigma}{\sigma} - \frac{1}{2} \frac{d\tau}{\tau} \right)$$

$$\frac{1}{\mu} = \frac{1}{G} \left( \frac{1}{2} \frac{d\sigma}{\sigma} + \frac{1}{2} \frac{d\tau}{\tau} \right)$$

where

$$\begin{aligned}
& \frac{1}{2} \left( \frac{\partial \varepsilon}{\partial t} \right)^2 \\
& \frac{1}{2} \left( \frac{\partial \varepsilon}{\partial t} \right)^2 \\
& \frac{1}{2} \left( \frac{\partial \varepsilon}{\partial t} \right)^2
\end{aligned}$$

This form has been integrated in  **$\theta$  - STOCK**.

## 9 DAMAGE MODELLING IN $\theta$ - STOCK

### 9.1 General formal frame of the model

In the following, a damage model dedicated to isothermal unsaturated porous media is presented. Irreversible thermodynamic processes induce irreversible strains. These dissipative phenomena may encompass plasticity and damage. For the sake of simplicity, irreversible deformations are presently supposed to be generated by damage only. The assumed split expression of incremental strains falls into:

$$d\underline{\underline{\varepsilon}} = d\underline{\underline{\varepsilon}}_{\underline{\underline{M}}}^{\text{rev}}(\underline{\underline{\Omega}}) + d\underline{\underline{\varepsilon}}_{\underline{\underline{S}}}^{\text{rev}}(\underline{\underline{\Omega}}) + d\underline{\underline{\varepsilon}}_{\underline{\underline{M}}}^{\text{irr}} + d\underline{\underline{\varepsilon}}_{\underline{\underline{S}}}^{\text{irr}} \quad (39)$$

in which  $\underline{\underline{\Omega}}$  is the damage variable, whose physical meaning is related to cracking. The microcracks damaging the sample are dispatched in crack families of approximately parallel directions. Three main orientations are retained. The damage developed in the Representative Elementary Volume is thus represented by three meso-cracks:

$$\underline{\underline{\Omega}} = \sum_{i=1}^3 d_i \underline{\underline{n}}_i \otimes \underline{\underline{n}}_i \quad (40)$$

$\underline{\underline{n}}_i$  is the unit vector normal to the  $i$ -th principal fracture plane,  $d_i$  is the crack density associated to the  $i$ -th crack family.  $d_i$  is related to the geometrical parameters of the fictive meso-cracks. Supposing that the REV is a cube of dimension  $b$ , and that meso-cracks are penny-shaped, with a radius  $r_i$  and an opening  $e_i$  :

$$d_i = \frac{V_i}{V_{REV}} = \frac{\pi \cdot (r_i)^2 \cdot e_i}{b^3} \quad (41)$$

Like in the former models integrated in **Θ-Stock** (Gatmiri [26,30,36]), reversible strains are related to the stress state variables by means of stiffness tensors:

$$\begin{cases} d\epsilon_{\underline{\underline{M}}}^{rev}(\underline{\underline{\Omega}}) = \underline{\underline{D}}_e^{-1}(\underline{\underline{\Omega}}) : d\sigma' \\ d\epsilon_{\underline{\underline{S}}}^{rev}(\underline{\underline{\Omega}}) = \underline{\underline{D}}_s^{-1}(\underline{\underline{\Omega}}) ds \end{cases} \quad (42)$$

The mechanical and suction rigidities  $\underline{\underline{D}}_e(\underline{\underline{\Omega}})$  and  $\underline{\underline{D}}_s(\underline{\underline{\Omega}})$  are made dependent on damage, in order to represent the mechanical degradation induced by cracking. Moreover, like in the preceding models developed in **Θ-Stock** for unsaturated porous media, reversible suction deformations are supposed to be isotropic:

$$d\epsilon_{\underline{\underline{S}}}^{rev}(\underline{\underline{\Omega}}) = \frac{d\epsilon_{S_v}^{rev}(\underline{\underline{\Omega}})}{3} \underline{\underline{Id}} = \frac{\beta_s^{-1}(\underline{\underline{\Omega}})}{3} \underline{\underline{Id}} \quad ds \quad (43)$$

with:

$$\underline{\underline{D}}_s(\underline{\underline{\Omega}}) = \beta_s(\underline{\underline{\Omega}}) \underline{\underline{Id}} \quad (44)$$

$$ds = \beta_s(\underline{\underline{\Omega}}) d\epsilon_{S_v}^{rev} \quad (45)$$

For the present damage model, it is furthermore assumed that total suction strains are isotropic:

$$d\epsilon_{\underline{\underline{S}}} = d\epsilon_{\underline{\underline{S}}}^{rev} + d\epsilon_{\underline{\underline{S}}}^{irr} = \frac{d\epsilon_{S_v}}{3} \underline{\underline{Id}} \quad (46)$$

The two conditions (43) and (46) lead to consider isotropic irreversible suction deformations also:

$$d\epsilon_{\underline{\underline{S}}}^{irr} = \frac{d\epsilon_{S_v}^{irr}}{3} \underline{\underline{Id}} \quad (47)$$

## 9.2 Phenomenological approach

The main thermodynamic requirements of the model are recalled in the works of Rice (Rice [40]), Hansen and Schreyer (Hansen and Schreyer [41]), and Collins and Houlsby (Collins and Houlsby [42]). As stated in the papers of Coussy and Dangla (Dangla et al., 1997 [43], Coussy and Dangla [44]), the In-

equality of Clausius-Duhem (ICD) for an unsaturated porous medium subjected to isothermal conditions writes:

$$\underline{\underline{\sigma}} : d\underline{\underline{\epsilon}} + p_w d\phi_w + p_g d\phi_g - d\psi_s(\underline{\underline{\epsilon}}, \phi_w, \phi_g) \geq 0 \quad (48)$$

in which  $\psi_s(\underline{\underline{\epsilon}}, \phi_w, \phi_g)$  is the free energy.  $\underline{\underline{\sigma}}$ ,  $p_w$  and  $p_g$  are the total stress tensor, the water pore pressure and the gas pore pressure respectively. The associated strain state variables are the total deformations  $\underline{\underline{\epsilon}}$ , the water content  $\phi_w$  and the gas content  $\phi_g$ . Fluid contents are defined as:

$$\phi_w = nS_w, \quad \phi_g = nS_g \quad (49)$$

in which  $n$  designates the total porosity of the medium,  $S_w$  and  $S_g$  being the water and the gas saturation degrees respectively. Both liquid and gas phases are supposed to saturate the pores of the material:

$$S_w + S_g = 1 \quad (50)$$

It is assumed that solid grains are incompressible. Volumetric deformations are thus generated by porosity variations only. With the convention of soil mechanics, based on positive compressions, this hypothesis leads to:

$$dn = -d\epsilon_v = -\text{Tr}(d\underline{\underline{\epsilon}}) = -\underline{\underline{\text{Id}}} : d\underline{\underline{\epsilon}} \quad (51)$$

The combination of equations (48-50) results in a new form of the ICD:

$$\underline{\underline{\sigma}} : d\underline{\underline{\epsilon}} + p_w d(nS_w) + p_g d(n - nS_w) - d\psi_s(\underline{\underline{\epsilon}}, \phi_w, \phi_g) \geq 0 \quad (52)$$

$$\underline{\underline{\sigma}} : d\underline{\underline{\epsilon}} + p_g dn - (p_g - p_w) d(nS_w) - d\psi_s(\underline{\underline{\epsilon}}, \phi_w, \phi_g) \geq 0 \quad (53)$$

$$(\underline{\underline{\sigma}} - p_g \underline{\underline{\text{Id}}}) : d\underline{\underline{\epsilon}} - (p_g - p_w) d(nS_w) - d\psi_s(\underline{\underline{\epsilon}}, \phi_w, \phi_g) \geq 0 \quad (54)$$

The assumption on solid incompressibility spares one degree of freedom: only two state variables instead of three are required for the model. The free energy turns to depend only on total strains and water content. Defining net stress as  $\underline{\underline{\sigma}}'' = \underline{\underline{\sigma}} - p_g \underline{\underline{\text{Id}}}$  and suction as  $s = p_g - p_w$ , inequality (54) becomes:

$$\underline{\underline{\sigma}}'' : d\underline{\underline{\epsilon}} - s d(nS_w) - d\psi_s(\underline{\underline{\epsilon}}, nS_w) \geq 0 \quad (55)$$

Due to the assumed split of deformations in  **$\Theta$ -Stock**, the strain state variables  $\underline{\underline{\epsilon}}$  and  $-nS_w$  are replaced by  $\underline{\underline{\epsilon}}_M$  and  $\underline{\underline{\epsilon}}_{S_v}$ . The ICD (55) for a damaged material thus writes:

$$\underline{\underline{\sigma}}'' : d\underline{\underline{\epsilon}}_{\underline{\underline{M}}} + s d\underline{\underline{\epsilon}}_{\underline{\underline{S_v}}} - d\underline{\underline{\psi}}_s(\underline{\underline{\epsilon}}_{\underline{\underline{M}}}, \underline{\underline{\epsilon}}_{\underline{\underline{S_v}}}, \underline{\underline{\Omega}}) \geq 0 \quad (56)$$

In the reversible domain, the free energy depends on the current damage level  $\underline{\underline{\Omega}}$  but does not evolve with  $\underline{\underline{\Omega}}$ , because damage is supposed to remain constant:  $d\underline{\underline{\Omega}} = 0$ . The thermodynamic conjugations relating stress- to strain- state variables are the following:

$$\begin{cases} \underline{\underline{\sigma}}'' = \frac{\partial \underline{\underline{\psi}}_s(\underline{\underline{\epsilon}}_{\underline{\underline{M}}}, \underline{\underline{\epsilon}}_{\underline{\underline{S_v}}}, \underline{\underline{\Omega}})}{\partial \underline{\underline{\epsilon}}_{\underline{\underline{M}}}} \\ \underline{\underline{s}} = \frac{\partial \underline{\underline{\psi}}_s(\underline{\underline{\epsilon}}_{\underline{\underline{M}}}, \underline{\underline{\epsilon}}_{\underline{\underline{S_v}}}, \underline{\underline{\Omega}})}{\partial \underline{\underline{\epsilon}}_{\underline{\underline{S_v}}}} \end{cases} \quad (57)$$

Moreover, a force variable associated to damage is defined:

$$\underline{\underline{Y}}_d = - \frac{\partial \underline{\underline{\psi}}_s(\underline{\underline{\epsilon}}_{\underline{\underline{M}}}, \underline{\underline{\epsilon}}_{\underline{\underline{S_v}}}, \underline{\underline{\Omega}})}{\partial \underline{\underline{\Omega}}} \quad (58)$$

The reduced dissipation inequality may be retrieved from equations (56-58):

$$\underline{\underline{Y}}_d : d\underline{\underline{\Omega}} \geq 0 \quad (59)$$

The following expression of the free energy is postulated, on the basis of the approach introduced by Dragon and Halm[45], Halm and Dragon[46]:

$$\underline{\underline{\psi}}_s(\underline{\underline{\epsilon}}_{\underline{\underline{M}}}, \underline{\underline{\epsilon}}_{\underline{\underline{S_v}}}, \underline{\underline{\Omega}}) = \underline{\underline{\psi}}_M^e(\underline{\underline{\epsilon}}_{\underline{\underline{M}}}, \underline{\underline{\Omega}}) + \underline{\underline{\psi}}_S^e(\underline{\underline{\epsilon}}_{\underline{\underline{S_v}}}, \underline{\underline{\Omega}}) + \underline{\underline{\psi}}_M^{\text{res}}(\underline{\underline{\epsilon}}_{\underline{\underline{M}}}, \underline{\underline{\Omega}}) + \underline{\underline{\psi}}_S^{\text{res}}(\underline{\underline{\epsilon}}_{\underline{\underline{S_v}}}, \underline{\underline{\Omega}}) \quad (60)$$

$\underline{\underline{\psi}}_M^e(\underline{\underline{\epsilon}}_{\underline{\underline{M}}}, \underline{\underline{\Omega}})$  and  $\underline{\underline{\psi}}_S^e(\underline{\underline{\epsilon}}_{\underline{\underline{S_v}}}, \underline{\underline{\Omega}})$  are damaged elastic deformation energies:

$$\underline{\underline{\psi}}_M^e(\underline{\underline{\epsilon}}_{\underline{\underline{M}}}, \underline{\underline{\Omega}}) = \frac{1}{2} \underline{\underline{\epsilon}}_{\underline{\underline{M}}} : \underline{\underline{D}}_e(\underline{\underline{\Omega}}) : \underline{\underline{\epsilon}}_{\underline{\underline{M}}} \quad (61)$$

$$\underline{\underline{\psi}}_S^e(\underline{\underline{\epsilon}}_{\underline{\underline{S_v}}}, \underline{\underline{\Omega}}) = \frac{1}{2} \underline{\underline{\epsilon}}_{\underline{\underline{S_v}}} : \underline{\underline{\beta}}_s(\underline{\underline{\Omega}}) : \underline{\underline{\epsilon}}_{\underline{\underline{S_v}}} \quad (62)$$

$\underline{\underline{\psi}}_M^{\text{res}}(\underline{\underline{\epsilon}}_{\underline{\underline{M}}}, \underline{\underline{\Omega}})$  and  $\underline{\underline{\psi}}_S^{\text{res}}(\underline{\underline{\epsilon}}_{\underline{\underline{S_v}}}, \underline{\underline{\Omega}})$  are potentials attesting the presence of residual deformations after

unloading, and are supposed to be linear functions of strain-state variables:

$$\underline{\underline{\psi}}_M^{\text{res}}(\underline{\underline{\epsilon}}_{\underline{\underline{M}}}, \underline{\underline{\Omega}}) = -\underline{\underline{g}}_M \underline{\underline{\Omega}} : \underline{\underline{\epsilon}}_{\underline{\underline{M}}} \quad (63)$$



$$\psi_s^{\text{res}}(\underline{\underline{\epsilon}}_{s_v}, \underline{\underline{\Omega}}) = -\underline{\underline{g}}_s \underline{\underline{\Omega}} : \underline{\underline{\epsilon}}_s = -\frac{\underline{\underline{g}}_s}{3} \text{Tr}(\underline{\underline{\Omega}}) \underline{\underline{\epsilon}}_{s_v} \quad (64)$$

$\underline{\underline{g}}_M$  and  $\underline{\underline{g}}_s$  are supposed to be constant material parameters. Using equations (57) and (60-64) to express the behaviour laws leads to:

$$\begin{cases} \underline{\underline{\sigma}}'' = \underline{\underline{D}}_e(\underline{\underline{\Omega}}) : \underline{\underline{\epsilon}}_{=M} - \underline{\underline{g}}_M \underline{\underline{\Omega}} \\ s = \beta_s(\underline{\underline{\Omega}}) \underline{\underline{\epsilon}}_{s_v} - \frac{\underline{\underline{g}}_s}{3} \text{Tr}(\underline{\underline{\Omega}}) \end{cases} \quad (65)$$

The damage-conjugated force is:

$$\underline{\underline{Y}}_d = -\frac{1}{2} \underline{\underline{\epsilon}}_{=M} : \frac{\partial \underline{\underline{D}}_e(\underline{\underline{\Omega}})}{\partial \underline{\underline{\Omega}}} : \underline{\underline{\epsilon}}_{=M} - \frac{1}{2} \underline{\underline{\epsilon}}_{s_v} : \frac{\partial \beta_s(\underline{\underline{\Omega}})}{\partial \underline{\underline{\Omega}}} \underline{\underline{\epsilon}}_{s_v} + \underline{\underline{g}}_M \underline{\underline{\epsilon}}_{=M} + \frac{\underline{\underline{g}}_s}{3} \underline{\underline{\epsilon}}_{s_v} \text{Id} \quad (66)$$

### 9.3 Computation of the irreversible strains by an associative damage flow rule

The incremental form of equations (65) is:

$$\begin{cases} d\underline{\underline{\sigma}}'' = \underline{\underline{D}}_e(\underline{\underline{\Omega}}) : d\underline{\underline{\epsilon}}_{=M}^{\text{rev}} + \underline{\underline{D}}_e(\underline{\underline{\Omega}}) : d\underline{\underline{\epsilon}}_{=M}^{\text{irr}} + \left( \frac{\partial \underline{\underline{D}}_e(\underline{\underline{\Omega}})}{\partial \underline{\underline{\Omega}}} : \underline{\underline{\epsilon}}_{=M} \right) : d\underline{\underline{\Omega}} - \underline{\underline{g}}_M d\underline{\underline{\Omega}} \\ ds = \beta_s(\underline{\underline{\Omega}}) d\underline{\underline{\epsilon}}_{s_v}^{\text{rev}} + \beta_s(\underline{\underline{\Omega}}) d\underline{\underline{\epsilon}}_{s_v}^{\text{irr}} + \left( \frac{\partial \beta_s(\underline{\underline{\Omega}})}{\partial \underline{\underline{\Omega}}} \underline{\underline{\epsilon}}_{s_v} \right) : d\underline{\underline{\Omega}} - \frac{\underline{\underline{g}}_s}{3} \text{Id} : d\underline{\underline{\Omega}} \end{cases} \quad (67)$$

Furthermore, the modelling assumptions (42) and (45) lead to the following equalities in the reversible domain:

$$\begin{cases} d\underline{\underline{\sigma}}'' = \underline{\underline{D}}_e(\underline{\underline{\Omega}}) : d\underline{\underline{\epsilon}}_{=M}^{\text{rev}} \\ ds = \beta_s(\underline{\underline{\Omega}}) d\underline{\underline{\epsilon}}_{s_v}^{\text{rev}} \end{cases} \quad (68)$$

The combination of systems (67) and (68) provides:

$$\begin{cases} d\underline{\underline{\epsilon}}_{=M}^{\text{irr}} = -\underline{\underline{D}}_e^{-1}(\underline{\underline{\Omega}}) : \left( \frac{\partial \underline{\underline{D}}_e(\underline{\underline{\Omega}})}{\partial \underline{\underline{\Omega}}} : \underline{\underline{\epsilon}}_{=M} \right) : d\underline{\underline{\Omega}} + \underline{\underline{g}}_M \underline{\underline{D}}_e^{-1}(\underline{\underline{\Omega}}) : d\underline{\underline{\Omega}} \\ d\underline{\underline{\epsilon}}_{s_v}^{\text{irr}} = -\beta_s^{-1}(\underline{\underline{\Omega}}) \left( \frac{\partial \beta_s(\underline{\underline{\Omega}})}{\partial \underline{\underline{\Omega}}} \underline{\underline{\epsilon}}_{s_v} \right) : d\underline{\underline{\Omega}} + \frac{\underline{\underline{g}}_s}{3} \beta_s^{-1}(\underline{\underline{\Omega}}) \text{Id} : d\underline{\underline{\Omega}} \end{cases} \quad (69)$$

Both incremental irreversible strain components may be computed if the increment of damage is known.  $d\Omega$  is determined by means of an associative flow rule. For this purpose, a yield function is expressed in the force-space:

$$f_d(\underline{\underline{\Omega}}, \underline{\underline{Y}}_d) = f_d(\underline{\underline{\Omega}}, \underline{\underline{Y}}_{d_1}^+) = \sqrt{\frac{1}{2} \text{Tr}(\underline{\underline{Y}}_{d_1}^+ \cdot \underline{\underline{Y}}_{d_1}^+)} - C_0 - C_1 \text{Tr}(\underline{\underline{\Omega}}) \quad (70)$$

$C_0$  is the initial damage threshold, and  $C_1$  controls the evolution rate of damage.  $\underline{\underline{Y}}_{d_1}^+$  is the damage-conjugated force associated to residual deformations due tensile loads:

$$\underline{\underline{Y}}_{d_1}^+ = g_M \underline{\underline{\varepsilon}}_M^+ + \frac{g_S}{3} \underline{\underline{\varepsilon}}_{S_v}^+ \quad \underline{\underline{Id}} = g_M \underline{\underline{\varepsilon}}_M^+ + g_S \underline{\underline{\varepsilon}}_S^+ \quad (71)$$

in which:

$$\underline{\underline{\varepsilon}}_J^+ = \sum_{k=1}^3 H(\underline{\underline{\varepsilon}}_{J_{kk}}) \underline{\underline{\varepsilon}}_{J_{kk}} \quad \underline{\underline{e}}_{J_k} \otimes \underline{\underline{e}}_{J_k}, \quad J = M, S \quad (72)$$

The  $\underline{\underline{e}}_{J_k}$  vectors are the principal directions of the deformation tensor  $\underline{\underline{\varepsilon}}_J$ . The  $\underline{\underline{\varepsilon}}_{J_{kk}}$  coefficients are the corresponding principal values of  $\underline{\underline{\varepsilon}}_J$ .  $H$  is the Heaviside function:

$$H(x) = \begin{cases} 0, & x \leq 0 \\ 1, & x > 0 \end{cases} \quad (73)$$

Supposing that the damage flow rule is associated leads to:

$$d\Omega = d\lambda_d \frac{\partial f_d(\underline{\underline{\Omega}}, \underline{\underline{Y}}_{d_1}^+)}{\partial \underline{\underline{Y}}_{d_1}^+} = d\lambda_d \frac{\underline{\underline{Y}}_{d_1}^+}{\sqrt{2 \text{Tr}(\underline{\underline{Y}}_{d_1}^+ \cdot \underline{\underline{Y}}_{d_1}^+)}} \quad (74)$$

in which  $d\lambda_d$  is the increment of damage multiplier, computed by means of the consistency equation

$$df_d = 0 :$$

$$d\lambda_d = - \frac{\frac{\partial f_d(\underline{\underline{\Omega}}, \underline{\underline{Y}}_{d_1}^+)}{\partial \underline{\underline{Y}}_{d_1}^+}}{\frac{\partial f_d(\underline{\underline{\Omega}}, \underline{\underline{Y}}_{d_1}^+)}{\partial \underline{\underline{\Omega}}} : \frac{\partial f_d(\underline{\underline{\Omega}}, \underline{\underline{Y}}_{d_1}^+)}{\partial \underline{\underline{Y}}_{d_1}^+}} : d\underline{\underline{Y}}_{d_1}^+ = \frac{\underline{\underline{Y}}_{d_1}^+ : d\underline{\underline{Y}}_{d_1}^+}{C_1 \underline{\underline{Id}} : \underline{\underline{Y}}_{d_1}^+} \quad (75)$$

#### 9.4 Calculation of the damaged rigidities by a micromechanical reasoning

At this stage, only the damaged stiffness  $\underline{\underline{D}}_e(\underline{\underline{\Omega}})$  and  $\beta_s(\underline{\underline{\Omega}})$  remain to be computed in order to get the complete expression of the additive breakdown of deformations exposed in equations (39), (42) and (43). For this purpose, the micromechanical approach consisting in applying the Principle of Equivalent Elastic Energy is adopted, and extended to suction. A damaged stress is defined as the stress undergone by the damaged material in a fictive intact state, characterized by the degraded material properties. It is better known in the literature as “effective stress”. A fourth-order operator  $\underline{\underline{M}}(\underline{\underline{\Omega}})$  relates the damaged net stress  $\underline{\underline{\hat{\sigma}}}$  to the real net stress  $\underline{\underline{\sigma}}$  :

$$\underline{\underline{\hat{\sigma}}} = \underline{\underline{M}}(\underline{\underline{\Omega}}) \underline{\underline{\sigma}} \quad (76)$$

In the present model, the following operator (Cordebois and Sidoroff [47]) is used:

$$\underline{\underline{\hat{\sigma}}} = (\underline{\underline{Id}} - \underline{\underline{\Omega}})^{1/2} \cdot \underline{\underline{\sigma}} \cdot (\underline{\underline{Id}} - \underline{\underline{\Omega}})^{1/2} \quad (77)$$

The definition (77) ensures the independence of the operator  $\underline{\underline{M}}(\underline{\underline{\Omega}})$  relatively to the behaviour law, and guaranties the symmetry of the damaged stress. Moreover, using this operator allows the derivation of the damaged stress from a thermodynamic potential (Lemaître and Desmorat [48]). The Principle of Equivalent Elastic Energy (Hansen and Schreyer [41]) postulates that the elastic deformation energy developed by the material in its real damaged state equals the elastic energy which would exist in the intact material, submitted to the damaged stress  $\underline{\underline{\hat{\sigma}}}$  :

$$\delta W_e(\underline{\underline{\hat{\sigma}}}, \underline{\underline{\Omega}} = 0) = \delta W_e(\underline{\underline{\sigma}}, \underline{\underline{\Omega}}) \quad (78)$$

Equality (78) may be translated as follows:

$$(\underline{\underline{\hat{\sigma}}}) : \underline{\underline{D}}_e^{-1}(\underline{\underline{\Omega}}) : d\underline{\underline{\sigma}} = (\underline{\underline{\hat{\sigma}}}) : \underline{\underline{D}}_e^{0-1} : d\underline{\underline{\hat{\sigma}}} \quad (79)$$

Assumption (79) leads to the following expression of the damaged mechanical stiffness  $\underline{\underline{D}}_e(\underline{\underline{\Omega}})$ :

$$\underline{\underline{D}}_e(\underline{\underline{\Omega}}) = \underline{\underline{M}}^{-1}(\underline{\underline{\Omega}}) : \underline{\underline{D}}_e^0 : \underline{\underline{M}}^{-T}(\underline{\underline{\Omega}}) \quad (80)$$

Developing relation (80) by inserting the expression of the operator of Cordebois and Sidoroff (77) leads to:

$$\underline{\underline{M}}^{-1}(\underline{\underline{\Omega}}) = \underline{\underline{\sigma}}'' \otimes \left[ \left( \underline{\underline{Id}} - \underline{\underline{\Omega}} \right)^{-1/2} \cdot \underline{\underline{\sigma}}'' \cdot \left( \underline{\underline{Id}} - \underline{\underline{\Omega}} \right)^{-1/2} \right]^T \quad (81)$$

Considering that suction effects are isotropic, the damaged suction is defined in the same way as in equations (76) and (77):

$$\text{Tr}(\hat{s} \cdot \underline{\underline{Id}}) = \text{Tr}(\underline{\underline{M}}(\underline{\underline{\Omega}}) : \underline{\underline{Id}} \cdot s) = s \cdot \text{Tr}(\left( \underline{\underline{Id}} - \underline{\underline{\Omega}} \right)^{1/2} \cdot \underline{\underline{Id}} \cdot \left( \underline{\underline{Id}} - \underline{\underline{\Omega}} \right)^{1/2}) \quad (82)$$

Developing relation (82) provides the following relation between the damaged and real suctions:

$$\hat{s} = \frac{s}{3} \cdot \text{Tr} \left[ \left( \underline{\underline{Id}} - \underline{\underline{\Omega}} \right)^{-1} \right] \quad (83)$$

Once again, the Principle of Equivalent Elastic Energy is applied in the domain of reversible strains. It is adapted to the concept of suction-related deformations:

$$\delta W_e(\hat{s}, \underline{\underline{\Omega}} = 0) = \delta W_e(s, \underline{\underline{\Omega}}) \quad (84)$$

which leads to:

$$\beta_s^{-1}(\underline{\underline{\Omega}}) \cdot ds = \beta_s^{0-1} \cdot \hat{s} d\hat{s} \quad (85)$$

Using relations (83) and (85) provides the expression of the damaged suction rigidity modulus

$$\beta_s(\underline{\underline{\Omega}}):$$

$$\beta_s(\underline{\underline{\Omega}}) = \frac{9\beta_s^0}{\left( \text{Tr} \left[ \left( \underline{\underline{Id}} - \underline{\underline{\Omega}} \right)^{-1} \right] \right)^2} \quad (86)$$

The complete behaviour law of the damaged unsaturated porous material is controlled by the break-down (39). Irreversible deformations are functions of the increment of damage (equations (69)), which is determined by an associative flow rule (equations (74) and (75)). Reversible strains depend on damaged rigidities (equations (42) and (44)), which are computed by applying the Principle of Equivalent Elastic Energy (expressions (81) and (86)). The coupled HHMD model is now complete. The remaining issue lies in fluid transfer problems.

### 9.5 Introduction of damage in the transfer laws

The gas diffusion model adopted in the preceding models programmed in **Θ-Stock** is the following (Gatmiri [27,36]):

$$\underline{v}_g = -\underline{K}_g \cdot \nabla \left( \frac{p_g}{\gamma_g} + z \right) \quad (87)$$

$$\underline{K}_g = b_g \frac{\gamma_g}{\mu_g} [e(1 - S_w)]^{\frac{1}{2}} \underline{Id} \quad (88)$$

$\gamma_g$  and  $\mu_g$  are the gas density and dynamic viscosity, respectively.  $b_g$  and  $c_g$  are material parameters, and  $z$  is the vertical coordinate or the current material point.

In compliance with the existing theoretical frame existing in **Θ-Stock**, water transfers are modelled by a Darcy law:

$$\underline{v}_w = -\underline{K}_w \cdot \nabla \left( \frac{p_w}{\gamma_w} + z \right) \quad (89)$$

The permeability tensor  $\underline{K}_w$  is split in an intrinsic part  $\underline{K}_{int}$  and a relative part  $k_r$ :

$$\underline{K}_w = k_r(S_w) \underline{K}_{int}(n, \underline{\Omega}) \quad (90)$$

The relative permeability reflects fluid properties only. Therefore, it does not depend on damage. It is assumed to be a function of the saturation degree, which may be computed either by the means of the equation of a state surface (Gatmiri et al, [19]), or, more simply, with the equation of a retention curve (Van Genuchten, [49]). Once the saturation degree is known, several integration types may be adopted to compute the relative permeability. Being damage-independent,  $k_r$  may be taken equal to the relative permeability of the intact material modelled in the former representations programmed in **Θ-Stock** (Gatmiri [26,30]):

$$k_r(S_w) = \left( \frac{S_w - S_{w,r}}{1 - S_{w,r}} \right)^d, \quad 3 < d < 4 \quad (91)$$

The intrinsic permeability  $\underline{\underline{K}}_{\text{int}}$  reflects the influence of the porous matrix on water transfers. That is why it is assumed to depend on deformations (through the total porosity  $\underline{n}$ ) and on damage, which are mechanical variables.  $\underline{\underline{K}}_{\text{int}}$  is split as follows:

$$\underline{\underline{K}}_{\text{int}}(\underline{n}, \underline{\underline{\Omega}}) = \underline{\underline{k}}_1(\underline{n}^{\text{rev}}, \underline{\underline{\Omega}}) + \underline{\underline{k}}_2(\underline{n}^{\text{frac}}, \underline{\underline{\Omega}}) \quad (92)$$

$\underline{n}^{\text{rev}}$  denotes the porosity related to reversible strains, and  $\underline{n}^{\text{frac}}$  is the porosity generated by crack opening.  $\underline{\underline{k}}_1(\underline{n}^{\text{rev}}, \underline{\underline{\Omega}})$  represents matrix transfer properties in the reversible domain, and is supposed equal to the intrinsic permeability of the intact material as formerly modelled in **Θ-Stock**:

$$\underline{\underline{k}}_1(\underline{n}^{\text{rev}}, \underline{\underline{\Omega}}) = k_0 10^{\alpha_k e^{\text{rev}}} \underline{\underline{Id}} \quad (93)$$

$k_0$  is a reference permeability, and  $\alpha_k$  is a material parameter.  $e^{\text{rev}}$  is the reversible void ratio. The expression of  $\underline{\underline{k}}_2(\underline{n}^{\text{frac}}, \underline{\underline{\Omega}})$  is derived from the permeability model dedicated to fractured rocks developed by Shao and his co-workers (Shao et al., [50]). The water flow which takes place inside a meso-crack is supposed to be laminar. For the  $i$ -th homogenized crack, the following cubic law may thus be used:

$$\underline{\underline{v}}_w^i(\underline{n}_i) = -\frac{1}{12\mu_w} (e_i)^3 (\underline{\underline{Id}} - \underline{n}_i \otimes \underline{n}_i) \nabla(p_w + \gamma_w z) \quad (94)$$

In the one hand, the total water flow existing in the cracks equals:

$$\underline{\underline{v}}_w^{\text{frac}} = \frac{1}{V_{\text{REV}}} \sum_{i=1}^3 (\underline{\underline{v}}_w^i(\underline{n}_i) V_i) \quad V_{\text{REV}} = b^3, \quad V_i = e_i \pi (r_i)^2 \quad (95)$$

In the other hand, the hypothesis of diffusive transfers provides:

$$\underline{\underline{v}}_w^{\text{frac}} = -\underline{\underline{k}}_2(\underline{n}^{\text{frac}}, \underline{\underline{\Omega}}) \nabla \left( \frac{p_w}{\gamma_w} + z \right) \quad (96)$$

The combination of equations (95) and (96) results in:

$$\underline{\underline{k}}_2(\underline{n}^{\text{frac}}, \underline{\underline{\Omega}}) = \frac{\gamma_w}{12\mu_w} \frac{\pi}{b^3} \sum_{i=1}^3 (e_i)^3 (r_i)^2 (\underline{\underline{Id}} - \underline{n}_i \otimes \underline{n}_i) \quad (97)$$

In order to ensure the validity of the concepts of Continuum Damage Mechanics, meso-cracks of the same orientation and belonging to distinct Volume Elements have to remain unconnected. Therefore:

$$\forall i, i = 1 \dots 3, \quad r_i < b \quad (98)$$

The matrix form of the described framework for modelling of the excavated damaged zone (EDZ) has been integrated in **Θ-Stock**.

## 10 APPLICATION AND RESULTS

Several validation tests have been performed and published ( Gatmiri et al [25,29,30], Gatmiri and Jenab-Vossoughi [28,32-34], Jenab-Vosoughi[38]). Three recent application cases are presented in the following.

### ***10.1 ONE DIMENSIONAL MODELING OF A HORIZONTAL CUT OF SOIL UNDER THERMAL LOADING***

In this case study, a special concept of waste disposal, currently used in France, has been investigated. In this concept, the cylindrical canisters, typically 0.7 m in diameter, are embedded vertically in small diameter well, which are related together by the lined galleries. The canister is assumed to be nearly rigid in comparison to the surrounding soils. The finite length of canister, which is on the order of 14 m long, is not considered in the analysis. An axisymmetric modeling is chosen. The vertical axis of the stocking well is considered as the axis of symmetry. The outer boundary of the soil is set at a radial distance of 200 m from the center of canister. The height of the elements is 2 m. Two types of materials are modeled in the mesh, from the 0.3 m engineered and geological barriers up to the outer boundary. Initial conditions (Stress, suction and temperature) have been determined by considering a depth of 500 m for this axisymmetric modeling.

- *Geometry*

The following dimensions are taken for the finite element model:

External radius of the mode                      Rext=200 m

Internal radius in the back of E.B.:        Rint=0.41 m

Thickness of E.B.:                      e=0.30 m

The rayon of excavated well:    Rexcav=0.71 m

- *Initial and Boundary Conditions:*

All initial and boundary conditions are illustrated in Fig. 5. In the table 1 the temperature flow as a function of time is given.

- *Mechanical, hydraulic and thermal parameters*

In this analysis a hyperbolic temperature-stress dependent model is used. In the tables 2, 3 and 4 the mechanical, hydraulic and thermal properties used in this modelling are presented.

- *Relative permeability and saturation degree state surfaces*

The relative water and air permeability curves are shown in Fig. 6. The state surfaces of the degree of saturation for the engineered and geological barriers are presented at two different temperatures, in Fig. 7.

- *Results and Interpretation*

This analysis is performed by using the linear and non linear temperature-stress dependent models. The results of the hyperbolic constitutive model analysis are presented here, in Figs. 8 to 12.

The profiles of radial displacements are shown for different instants in Fig. 8. The maximum of observed displacement is about 28 mm, which can be clearly higher than the same value obtained with a linear analysis. We should indicate that this maximum value is observed later in the linear model. This delay is due to pore pressure dissipation.

The temperature profiles presented in Fig. 9 do not indicate a significant difference between the results provided by the non linear and linear models (performed but not presented here). This confirms that the thermal kinematics is independent of the mechanical behavior. The pore water and air pressure profiles in different instants are shown in Figs. 10 and 11, respectively. The profiles of suction along the model at different times are presented in Fig. 12.

## ***10.2 Two-dimensional modeling***

The results of the application of this model to a laboratory test Villar et al. [51] is presented hereafter. In this numerical analysis, displacements and transfers in the soil sample are studied. The overall configuration is shown in Fig. 13. Details concerning the experimental device and initial and boundary



conditions can be found in Gatmiri et al. [27,28]. The required parameters have been determined from experimental results reported by Villar et al. [51] and are as the following:

- thermal parameters;

$C_s = 800 \text{ J/kgK}$ ,  $C_w = 4180 \text{ J/kgK}$ ,  $C_v = 1870 \text{ J/kgK}$ ,  $C_g = 1000 \text{ J/kgK}$ ,  $\lambda_s = 0.9 \text{ W/mK}$ ,  $\lambda_w = 0.6 \text{ W/mK}$ ,  $\lambda_a = 0.0258 \text{ W/mK}$ ,  $h_{fg} = 2.4 \times 10^6 \text{ J/kg}$  (Villar et al. [51]),

- Air permeability parameters;

$c = 3.0 \times 10^{-10}$  ;  $d = 4.0$  ;  $\mu_g = 1.846 \times 10^{-5} \text{ kPa s}$ ,

- Water permeability parameters (Villar et al., [51]);

$a = 1.2 \times 10^{-9}$  ;  $\alpha = 5.0$  ;  $S_{ru} = 0.05$ , Variations of the water and air permeabilities with temperature and degree of saturation are presented in Figs. 14 and 15.

- Parameters for thermal state surface of degree of saturation;

$a_s = 1.0$  ;  $b_s = -2.088 \times 10^{-8}$  ;  $c_s = 2.08855 \times 10^{-4}$  ;  $d_s = 1. \times 10^{-5}$ . A presentation of this surface is given in Fig. 16. The void ratio state surface is also presented in Fig. 17 for two different temperatures.

As the thermo-hydro-mechanical behaviour is investigated here, simulation results in temperature, degree of saturation, void ratio and suction are presented (Figs. 18 - 21) for a vertical section of the cylindrical cell, at the end of the test. It is observed that numerical results are quite compatible with experimental ones and this model can provide satisfactory prediction of the behavior.

### ***10.3 Elastoplastic two-dimensional modeling of nuclear waste disposal***

A real case of nuclear waste disposal has been considered. Host rock is Argillite and engineered barrier is MX80 that is an expansive clay used in galleries and wells between the canister and geological barrier. The geometry and mesh are illustrated in Fig. 22. The mesh is constituted of 1638 quadrilateral elements and 1773 nodes. Fig. 22 shows the general boundary condition too. Initial stresses, degree of saturation, void ratio and temperature are shown in Fig. 23. Fig. 24 illustrates the seven points in the Argillite and MX80 for which the results are presented. Degree of saturation state surfaces (Gatmiri [26, 35]) used in this analysis are matched to the Van Genuchten water retention curves measured for the Argillite and MX80 (See Figs. 25 and 26). The variation of air and water permeabilities versus the degree of saturation for Argillite and MX80 are presented in Figs. 25 and 26. Figs. 27 and 28 present the state surface of degree of saturation for Argillite and MX80. The thermoelastoplastic model described in section 8.1 and

integrated in  $\Theta$ -STOCK has been used in this analysis. The parameters of elastoplastic model for Argillite and MX80 are given in table 5 and 6. Tables 7 and 8 present the material and water properties, respectively.

The results of analysis are presented in Figs 29-35. Temperature and suction distribution are illustrated in Figs 29 and 30, respectively. Time evolution of radial displacement in the massif is presented in Fig. 31. Figs. 31 to 35 illustrate the stress paths for argillite and MX80 in p-q and p-s coordinates, respectively.

## 11 CONCLUSIONS

A theoretical framework for the analysis of fully coupled moisture, heat, gas and skeleton deformation is established for an unsaturated field. The new theoretical formulation is a combination of two extended theories; the first part is an extension of the moisture transfer theory of Philip and de Vries. The second part is the extension of the isothermal deformation theory of unsaturated soil to thermal effects. A complete set of equations is presented, in which the suction-based equations of moisture, heat and air transport are combined with the equilibrium equation of the solid skeleton and in which the constitutive law relation is combined with the equations of the void ratio and degree of saturation hyper state surfaces. These state surfaces are temperature-dependent.

A good agreement between the predictions of this new model and experimental results reported by others has shown the strong ability of this new model, which is encouraging.

## REFERENCES

- [1] Philip JR, de Vries D. A. Moisture Movement in porous materials under temperature gradients'. Trans. Am. Geophys. Un. 1957;38:222-232.
- [2] de Vries D. A. Simultaneous transfer of heat and moisture in porous media. Trans. Am. Geophys. Un. 1958;39(5):909-916.
- [3] Taylor SA, Cary JW. Linear equations for the simultaneous flow of matter and energy in a continuous soil system. Soil Science Society of America 1964; Proc. 28:167-172.
- [4] Cassel DK, Nielsen DR, Biggar JW. Soil-Water movement in response to Imposed temperature gradients. Soil Science Society of America 1969; Proc. 33:493-500.
- [5] Dirksen C. Water movement and frost heaving in unsaturated soil without an external source of water. PhD. Dissertation, Cornell University, 1964.
- [6] Sophocleous M. Analysis of water and heat flow in unsaturated-saturated porous media. Water Resources Research 1979;15(5):1195-1206.
- [7] Milly PCD. Moisture and heat transport in hysteretic, inhomogeneous porous media : A matric heat-based formulation and a numerical model. Water Resources Research 1982;18(3):489-498.
- [8] Thomas HR. Nonlinear analysis of heat and moisture transfer in unsaturated soil. Journal of Engineering Mechanics ASCE 1987;113(8):1163-1180.

- [9] Thomas HR, He Y. Analysis of coupled heat, moisture and air transfer in a deformable unsaturated soil. *Géotechnique* 1995;45:677-689.
- [10] Geraminegad M, Saxena SK. A coupled thermoelastic model for saturated-unsaturated porous media. *Géotechnique* 1986;36(4):539-550.
- [11] Coleman JD. Stress strain relations for partly saturated soil, Correspondence. *Géotechnique* 1962;12(4):348-350.
- [12] Bishop AW, Blight GE. Some aspects of effective stress in saturated and partly saturated soils. *Géotechnique* 1963;13(3):177-197.
- [13] Fredlund DG, Morgenstern NR. Stress state variables for unsaturated soils. *J. Geotech. Engng Am. Soc. Civ. Engrs* 1977;103(5):447-466.
- [14] Fredlund DG, N.R. Morgenstern NR. Constitutive relations for volume change in unsaturated soil. *Can. Geotech. J.* 1976;13(3):261-276.
- [15] Fredlund DG. Appropriate concepts and technology for unsaturated soils. *Can. Geotech. J.* 1979;16:121-139.
- [16] Matyas EL, Radhakrishna HS. Volume change characteristics of partially saturated soils. *Géotechnique* 1968;18:432-448.
- [17] Lloret A, Alonso EE. Consolidation of unsaturated soils including swelling and collapse behaviour. *Géotechnique* 1980;30(4):449-477.
- [18] Alonso EE, Battle F, Gens A, Lloret A. Consolidation analysis of partially saturated soils. Application to earth dam construction. *Proc. Int. Conf. on Numerical Methods in Geotechnics*, Innsbruck, 1988. p. 1303-1308.
- [19] Gatmiri B. Surfaces d'états et déformation des barrages en remblai avec drains sous pression négative. CERMES Activity Report (ENPC), 1994.
- [20] Gatmiri B, Delage P. Nouvelle formulation de la surface d'état en indice des vides pour un modèle non linéaire élastique des sols non saturés. *Proc. 1st Int. Con. Unsaturated Soils*, 1995;2:1049-1056.
- [21] Nanda A. Analysis of consolidation of embankment dams during construction. CERMES Activity Report (ENPC), 1989.
- [22] Gatmiri B. Evolution du code U-DAM ; Description détaillée et mode d'emploi. CERMES Activity Report (ENPC), 1992.
- [23] Gatmiri B. Validation du code U-DAM. CERMES Activity Report (ENPC), 1993.
- [24] Gatmiri B, Delage P, Cerrolaza M. UDAM: powerful finite element software for the analysis of unsaturated porous media. *International Journal of Advances in Engineering Software* 1998;29(1):29-43.
- [25] Gatmiri B, Tavakoli S, Moussavi J, Delage P. Numerical approach of elastoplastic consolidation of unsaturated soils. *First International Conference on Unsaturated Soils*, Paris, France, 1995. p 1057-1064.
- [26] Gatmiri B. Analysis of fully coupled behavior of unsaturated porous media under stress, suction and temperature gradient. Final report of CERMES-EDF, 1997.
- [27] Gatmiri B, Seyedi M, Delage P, Fry JJ. A new suction-based mathematical model for thermo-hydro-mechanical behavior of unsaturated porous media. NUMOG VI, Quebec, Canada, 2-4 July 1997. p. 291-296.
- [28] Gatmiri B, Jenab-Vossoughi B, Delage P. Validation of  $\theta$  - STOCK, finite element software for the analysis of thermo-hydro-mechanical behaviour of engineered clay barriers. *Proceedings of NAFEMS WORLD CONGRESS 99 on Effective Engineering Analysis*, 1999;1:645-656.
- [29] Gatmiri B. Thermo-hydro-mécanique des sols saturés et non saturés dans le Code\_Aster, Final report of CERMES-EDF, 2000.
- [30] Gatmiri B. Framework of a non linear fully coupled thermo-hydro-mechanical behavior of unsaturated porous media. Keynote lecture of the 3rd Iranian International Conference on Geotechnical Engineering and Soil Mechanics December, Tehran, Iran, 9-11, 2002.
- [31] Gatmiri B, Delage P. A formulation of fully coupled thermal-hydraulic-mechanical behavior of saturated porous media - numerical approach. *Int. J. Numer. Anal. Methods Geomech.* 1997;21(3):199-225.
- [32] Gatmiri B, Jenab B. On the effects of Parameters in a nonlinear Thermo-Hydro-Mechanical soil model. 4th European Conf. on Numerical Methods in Geotech. Engineering, Udine, Italy, 14-16 October, 1998. p. 293-303.
- [33] Gatmiri B, Jenab-Vossoughi B. Effects of heat convection and phase changes on heat and fluid transfer in unsaturated porous media. *Heat Transfert 2000*, Madrid, 26-28 June 2000, 6p.
- [34] Gatmiri B, Jenab-Vossoughi B. Effects of heat convection and phase changes on heat and fluid transfer in unsaturated porous media. *UNSAT 2002*, Recife, Brazil, 2002. p. 77-82.

- [35] Gatùiri B, Hoor A. Finite Element Method And Modelling of Thermo-Hydro-Mechanical Behaviour Of Nuclear Waste Repositories, 11th International Conference of IACMAG, Turin, Italy, June 2005;3:159-166.
- [36] Gatmiri B, Horr A. Excavation effect on the thermo-hydro-mechanical behaviour of a geological barrier. *Physics and Chemistry of the Earth* 2007;32(8-14):947-956.
- [37] Gatmiri B, Magnin P. Minimum time step criterion in FE analysis of unsaturated consolidation: Model UDAM. *Proceeding 3<sup>rd</sup> European Spec. Conf. on Num. Meth. in Geo. Eng.*, Manchester, UK, 1994.
- [38] Jenab-Vossoughi B. Etude numérique de la modélisation thermo-élasto-plastique des sols non saturés”, PhD Dissertation, Ecole Nationale des Ponts et Chaussées, 2000, 253p.
- [39] Gatmiri B, Seyedi M. Thermohydromechanical behaviour of non linear and inelastic saturated porous media. 6th International Workshop on Key Issues in Wastes Isolation research (KIWIR), Paris, 28-30 November 2001. p. 423-463.
- [40] Rice JR. Inelastic constitutive relations for solids: an internal-variable theory and its application to metal plasticity. *Journal of the Mechanics and the Physics of Solids* 1971;19:433-455.
- [41] Hansen NR, Schreyer HL. A thermodynamically consistent frame-work for theories of elastoplasticity coupled with damage. *Int. J. Solids and Structures* 1994;31(3):359-389.
- [42] Collins IF, Houlsby GT. Application of thermomechanical principles to the modelling of geotechnical materials. *Proceedings Mathematical, Physical and Engineering Sciences* 1997;453(1964):1975-2001
- [43] Dangla P, Malinsky L, Coussy O. Plasticity and imbibition-drainage curves for unsaturated soils: a unified approach. In: Pietruszczak, Pande, editors. *Proc. Numerical Models in Geomechanics*. Balkema, Rotterdam, 1997. p. 141-146.
- [44] Coussy O, Dangla P. Approche énergétique du comportement des sols non saturés. In: Coussy O, Fleureau JM, editors. *Mécanique des sols non saturés*. Hermes publishing company, 2002. p. 137-174.
- [45] Dragon A, Halm D. Modélisation de l'endommagement par méso-fissuration : comportement unilatéral et anisotropie induite. *C.R. Acad. Sci. Paris* 1996;T.322(IIb):275-282.
- [46] Halm D, Dragon A. An anisotropic model of damage and frictional sliding for brittle materials. *Eur. J. Mech. A/ Solids* 1998;17(3):439-460.
- [47] Cordebois JP, Sidoroff F. Endommagement anisotrope en élasticité et plasticité. *Journal de Mécanique théorique et appliquée* 1982; spec. issue:45-60.
- [48] Lemaître J, Desmorat R. *Engineering damage mechanics - ductile, creep and fatigue failures*. Springer-Verlag, Berlin Heidelberg, 2005, 395p.
- [49] Van Genuchten MT. A closed-form equation for predicting the hydraulic conductivity of unsaturated soils. *Soil Science Society of America Journal* 1980;44:892-898.
- [50] Shao JF, Zhou H, Chau KT. Coupling between anisotropic damage and permeability variation in brittle rocks. *International Journal for Numerical and Analytical Methods in Geomechanics* 2005;29:1231-1247.
- [51] Villar MV, Cuevas J, Fernandez AM, Martin PL. Effects of the interaction of heat and water flow in compacted bentonite. *Proceedings of International workshop thermomechanics of clays and clay barriers (ISMES)*, Bergamo, 1993.

## Appendix 1

### Notations:

#### *Latin letters*

$a_e$ ,  $b_e$ ,  $c_e$ ,  $a_s$ ,  $b_s$ ,  $c_s$  and  $d_s$  : constants used in state surfaces formulation.

$B$  : bulk modulus

$b_i$  : body force

$C_{PW}$  : specific heat capacity of liquid

$C_{PV}$  : specific heat capacity of vapor

$C_{Pg}$  : specific heat capacity of gas

$D$  : elasticity matrix

$D_W$  : gravitational diffusivity

$D_T$  : thermal moisture diffusivity and is equal to  $D_{TV}+D_{TW}$ ,

$D_o$  : isothermal moisture diffusivity and is equal to  $D_{ov}+ D_{ow}$ .

$E$  : tangent elastic modulus

$e$  : void ratio

$e_0$  : initial void ratio

$g$  : gravity acceleration

$H$  : Henry's constant

$h_{fg}$  : latent heat of vaporization of soil water

$K_g$  : gas permeability

$K_b$ ,  $K_L$ ,  $K_u$  : modulus numbers (dimensionless) used in hyperbolic model

$m$  : constant used in definition of constitutive law

$n$  : porosity

$n$  : constant used in hyperbolic model

$p_{\text{atm}}$  : atmosphere pressure

$P_g$  : gas pressure

$P_w$  : pore water pressure

$Q$  : heat flow

$q$  : vector of water flow

$R_f$  : constant used in hyperbolic model

$S_r$  : degree of water saturation

$T$  : temperature

$T_0$  : arbitrary reference temperature

$t$  : time

$U$  : liquid velocity

$V$  : vapour velocity

$V_g$  : vector of gas velocity

$Z, z$  : elevation

*Greek letters*

$\delta_{ij}$  : Kronecker delta

$\epsilon$  : strain tensor

$\Phi$  : the volumetric bulk heat content of medium

$\gamma_g$  : specific weight of gas

$\lambda$  : Fourier heat diffusion coefficient of unsaturated mixture

$\theta_w, \theta$  : volumetric water content,  $\theta_w = n S_r$

$\rho_g$  : density of gas

$\rho_m$  : density of moisture

$\rho_w$  : density of liquid

$\rho_v$  : density of water vapor, kgm / m<sup>3</sup>

$\sigma_{ij}$  : stress tensor

$\sigma_c$  : preconsolidation stress

## Appendix 2

Integral form of the matrices are followings:

$$[R] = \int_{\Omega} B^T \cdot D \cdot B d\Omega$$

$$[C_T] = + \int_{\Omega} B^T \cdot C \cdot N d\Omega$$

$$[C_w] = - \int_{\Omega} B^T \cdot F \cdot N d\Omega$$

$$[C_g] = \int_{\Omega} B^T (m - F) \cdot N d\Omega$$

$$\{F_o\} = \int N^T \cdot \bar{\sigma} \cdot d_{\Gamma} + \int N b_i d\Omega$$

$$[C_{TU}] = \int_{\Omega} N^T [D_{3U}] B d\Omega \quad \text{with : } [D_{3U}] = [m^T [IV] + \underline{g}_1 [V] D]$$

$$[C_{TT}] = \int_{\Omega} N^T [D_{3T}] N d\Omega \quad \text{with: } [D_{3T}] = [(g_3 - C \underline{g}_1) [V] + [VI]]$$

$$[C_{Tw}] = \int_{\Omega} N^T [D_{3w}] N d\Omega \quad \text{with : } [D_{3w}] = [(\underline{g}_1 F - g_2) [V]]$$

$$[C_{Tg}] = \int_{\Omega} N^T [D_{3Pg}] N d\Omega \quad \text{with: } [D_{3Pg}] = [(g_2 - F \underline{g}_1) [V]]$$

$$[K_{TT}] = \int_{\Omega} (\nabla N)^T \left[ \lambda + [fx1] (T - T_0) + \rho_w D_{Tv} h_{fg} + \rho_v K_g \beta_{Pg} h_{fg} \right] \nabla N d\Omega$$

$$fx1 = \rho_w C_w D_{Tw} + \rho_w C_v D_{Tv} + \rho_g K_g \beta_{Pg} C_{Pg}$$

$$[K_{Tw}] = \int_{\Omega} (\nabla N)^T \left[ (\rho_w C_w D_{Pw} + \rho_w C_v D_{Pv}) (T - T_0) + \rho_w D_{Pv} h_{fg} \right] \nabla N d\Omega$$

$$[K_{Tg}] = \int_{\Omega} (\nabla N)^T \left[ (C_g K_g \rho_g (T - T_0) + \rho_v K_g h_{fg}) \right] \nabla N d\Omega$$



$$\{F_T\} = \int_{\Omega} (\nabla N)^T [C_w \rho_w (T - T_0) K_0] \nabla Z d\Omega + \int_{\Gamma} N^T q_h d_{\Gamma}$$

$$[C_{wv}] = \int_{\Omega} N^T [A m^T + B' \underline{g}_1 D] [B] d\Omega$$

$$[C_{wT}] = \int_{\Omega} N^T [E + B' (g_3 - \underline{g}_1 C) + n S_r \beta_T] N d\Omega$$

$$[C_{ww}] = \int_{\Omega} N^T [B' (\underline{g}_1 F - g_2) + n S_r \beta_p] N d\Omega$$

$$[C_{wg}] = \int_{\Omega} N^T [B' (g_2 - \underline{g}_1 F)] N d\Omega$$

$$[K_{wT}] = \int_{\Omega} (\nabla N)^T [D_{TT}] \nabla N d\Omega \quad \text{with : } D_{TT} = \rho_w (D_{Tv} + D_{Tw})$$

$$[K_{ww}] = \int_{\Omega} (\nabla N)^T [D_p] \nabla N d\Omega \quad \text{with : } D_p = \rho_w (D_{pv} + D_{pw})$$

$$\{F_w\} = \int_{\Omega} (\nabla N)^T [K_{\theta}] \nabla N d\Omega - \int_{\Gamma} N^T q_w d_{\Gamma} - \int_{\Gamma} N^T q_v d_{\Gamma} \quad \text{with : } K_{\theta} = \rho_w D_w$$

$$[C_{gu}] = \int_{\Omega} N^T [D_{2u}] [B] d\Omega ; D_{2u} = \left[ m^T \rho_g (1 - S_r (1 - H)) + [\alpha_{sr} \underline{g}_1 + (1 - H) n \rho_g] \cdot D \right]$$

$$[C_{gT}] = \int_{\Omega} N^T [n(1 - S_r (1 - H)) \alpha_T + (g_3 - \underline{g}_1 C) [\alpha_{sr} - (1 - H) n \rho_g]] N d\Omega$$

$$[C_{gw}] = \int_{\Omega} N^T [(\underline{g}_1 F - g_2) (\alpha_{sr} - (1 - H) n \rho_g)] N d\Omega$$

$$[C_{gg}] = \int_{\Omega} N^T [n(1 - S_r (1 - H)) \alpha_p + (g_2 - \underline{g}_1 F) (\alpha_{sr} - (1 - H) n \rho_g)] N d\Omega$$

$$[K_{gT}] = \int_{\Omega} (\nabla N^T) \left[ \frac{-K_g \rho_g}{\gamma_g} \beta_{pg} - H \rho_a D_{Tw} + \rho_w D_{Tv} \right] \nabla N d\Omega$$

$$\left[ \mathbf{K}_{\text{gw}} \right] = \int_{\Omega} (\nabla \mathbf{N})^T \left[ \rho_{\text{w}} \mathbf{D}_{\text{pv}} - H \rho_{\text{a}} \mathbf{D}_{\text{aw}} \right] \nabla \mathbf{N} d\Omega$$

$$\left[ \mathbf{K}_{\text{gg}} \right] = \int_{\Omega} (\nabla \mathbf{N})^T \left[ \frac{-\mathbf{K}_{\text{g}}}{\gamma_{\text{g}}} \rho \mathbf{g} \right] \nabla \mathbf{N} d\Omega$$

$$\left\{ \mathbf{F}_{\text{g}} \right\} = \int_{\Omega} (\nabla \mathbf{N})^T \left[ H \rho_{\text{a}} \mathbf{K}_{\text{th}} + \rho_{\text{g}} \mathbf{K}_{\text{g}} \right] \nabla Z + \int_{\Gamma} \mathbf{N}^T \mathbf{q}_{\text{v}} d_{\Gamma} - \int_{\Gamma} \mathbf{N}^T \mathbf{q}_{\text{g}} d_{\Gamma}$$

In which the following terms are used :

$$\mathbf{F} = \mathbf{D} \mathbf{D}_s^{-1} \quad \text{with} \quad \mathbf{D}_s^{-1} = \beta_s \mathbf{m} \quad \text{in which} \quad \beta_s = \frac{1}{1 + e} \frac{\partial e}{\partial (\mathbf{p}_{\text{g}} - \mathbf{p}_{\text{w}})}$$

$$\text{and } \mathbf{m}^T = \begin{bmatrix} 1 & 1 & 0 \end{bmatrix}$$

$$\mathbf{C} = \mathbf{D} \mathbf{D}_t^{-1} \quad \text{with} \quad \mathbf{D}_t^{-1} = \beta_t \mathbf{m} \quad \text{in which} \quad \beta_t = \frac{1}{1 + e} \frac{\partial e}{\partial T}$$

$$\underline{\mathbf{g}}_1 = \frac{\partial \mathbf{S}_{\text{r}}}{\partial \left( \boldsymbol{\sigma} - \mathbf{P}_{\text{g}} \right)}$$

$$\underline{\mathbf{g}}_2 = \frac{\partial \mathbf{S}_{\text{r}}}{\partial \left( \mathbf{P}_{\text{g}} - \mathbf{P}_{\text{w}} \right)}$$

$$\underline{\mathbf{g}}_3 = \frac{\partial \mathbf{S}_{\text{r}}}{\partial T}$$

$$\underline{\mathbf{g}}_1 = \mathbf{m}_1^T \cdot \mathbf{g}_1 = \begin{bmatrix} 0 & 1 & 0 \end{bmatrix} \mathbf{g}_1$$

$$\alpha_{\text{T}} = \frac{\rho_{\text{g}}}{T + 273}$$

$$\alpha_{\text{p}} = \frac{\left( 1 + \frac{H \mathbf{S}_{\text{r}}}{1 - \mathbf{S}_{\text{r}}} \right)}{\mathbf{R}_{\text{g}} (T + 273)}$$

$$\alpha_{\text{Sr}} = \frac{\text{P}_{\text{g}} + \text{P}_{\text{atm}}}{\text{R}_{\text{g}}(\text{T} + 273)} \frac{\text{H}}{(1 - \text{S}_{\text{r}})^2}$$

$$\text{A} = \rho_{\text{w}}\text{S}_{\text{r}} + \rho_{\text{v}}\big(1 - \text{S}_{\text{r}}\big) + \text{nS}_{\text{r}}\big(1 - \text{S}_{\text{r}}\big)\text{A}_{\text{n}}$$

$$\text{B}' = \text{n}\big(\rho_{\text{w}} - \rho_{\text{v}}\big) + \text{n}^2\big(1 - \text{S}_{\text{r}}\big)\text{A}_{\text{n}}$$

$$\text{E} = \text{n}\big(1 - \text{S}_{\text{r}}\big)\big(\rho_{\text{v}}\text{A}_0 - 4975.9\text{nS}_{\text{r}}\text{A}_{\text{n}}\big)$$

$$\beta_{\text{T}} = \left.\frac{\partial \rho_{\text{w}}}{\partial \text{T}}\right|_{\text{P}_{\text{w}}=\text{cte}}, \quad \beta_{\text{P}} = \left.\frac{\partial \rho_{\text{w}}}{\partial \text{P}_{\text{w}}}\right|_{\text{T}=\text{cte}}$$

$$\rho_{\text{w}} = \rho_{\text{w}0}\big(1 + \beta_{\text{P}}\rho_{\text{w}} + \beta_{\text{T}}\text{T}\big)$$

$$\text{I} = \text{S}_{\text{r}}\rho_{\text{w}}\text{C}_{\text{Pw}} - \rho_{\text{s}}\text{C}_{\text{Ps}} + \big(1 - \text{S}_{\text{r}}\big)\big(\rho_{\text{v}}\text{C}_{\text{Pv}} + \rho_{\text{g}}\text{C}_{\text{Pg}}\big) + \text{A}_{\text{n}}\text{S}_{\text{r}}\text{n}\big(1 - \text{S}_{\text{r}}\text{C}_{\text{Pv}}\big)$$

$$\text{II} = \text{n}\rho_{\text{w}}\text{C}_{\text{Pw}} - \text{n}\big(\rho_{\text{v}}\text{C}_{\text{Pv}} + \text{C}_{\text{Pg}}\rho_{\text{g}}\big) + \text{A}_{\text{n}}.\text{n}^2\big(1 - \text{S}_{\text{r}}\big)\text{C}_{\text{Pv}}$$

$$\text{III} = \big(\big(\text{A}_0\rho_{\text{v}} - 4975.9\text{nS}_{\text{r}}\text{A}_{\text{n}}\big)\text{n}\big(1 - \text{S}_{\text{r}}\big)\text{C}_{\text{Pv}}\big)$$

$$\text{IV} = \text{I}\big(\text{T} - \text{T}_0\big) + \big(1 - \text{S}_{\text{r}}\big)\rho_{\text{v}}\text{h}_{\text{fg}} + \text{n}\big(1 - \text{S}_{\text{r}}\big)\text{h}_{\text{fg}}\text{A}_{\text{n}}.\text{S}_{\text{r}}$$

$$\text{V} = \text{II}\big(\text{T} - \text{T}_0\big) - \text{n}\rho_{\text{v}}\text{h}_{\text{fg}} + \text{n}^2\big(1 - \text{S}_{\text{r}}\big)\text{h}_{\text{fg}}.\text{A}_{\text{n}}$$

$$\text{VI} = \text{C}_{\text{T}} + \text{III}\big(\text{T} - \text{T}_0\big) + \text{n}\big(1 - \text{S}_{\text{r}}\big)\text{h}_{\text{fg}}\big(\text{A}_0\rho_{\text{v}} - 4975.9\text{nS}_{\text{r}}\text{A}_{\text{n}}\big)$$

$$\text{A}_0 = \frac{1}{\rho_0} \frac{\text{d}\rho_0}{\text{d}\text{T}}$$

$$\text{A}_{\text{n}} = \frac{1}{\text{S}_{\text{r}}} \frac{\partial \rho_{\text{v}}}{\partial \text{n}} = \frac{1}{\text{n}} \frac{\partial \rho_{\text{v}}}{\partial \text{S}_{\text{r}}}$$

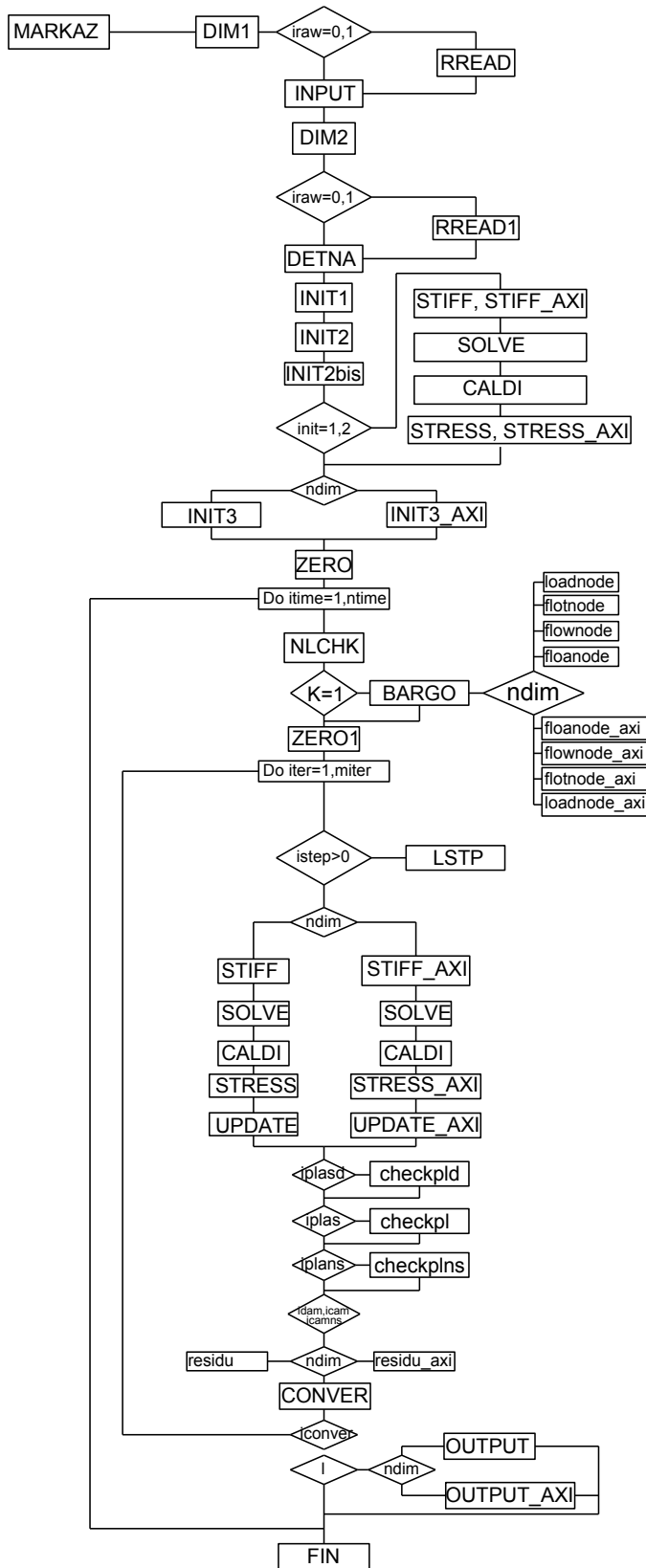


Fig. 1: Global flow-chart of finite element package  $\theta$  - *STOCK*

F

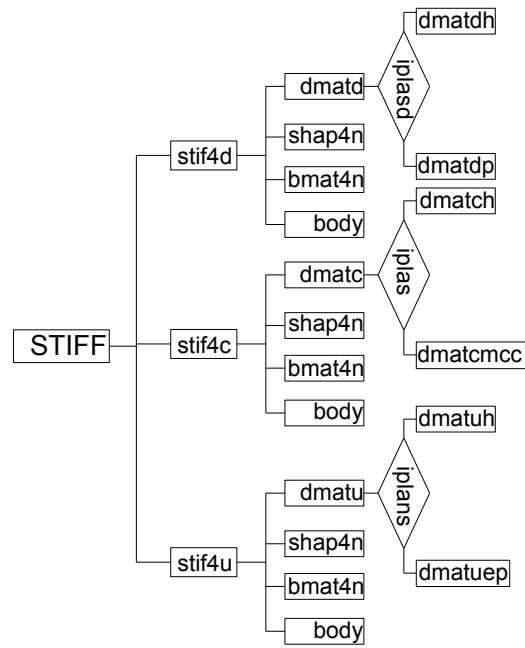


Fig. 2: Flow-chart to compute the stiffness matrices for three element types in plain strain module

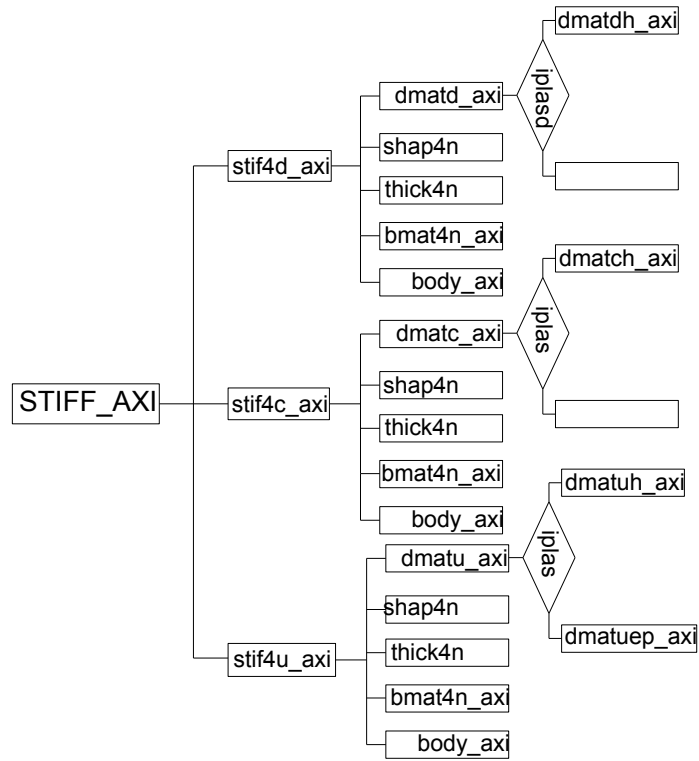


Fig. 3: Flow-chart to compute the stiffness matrices for three element types in axisymmetric module

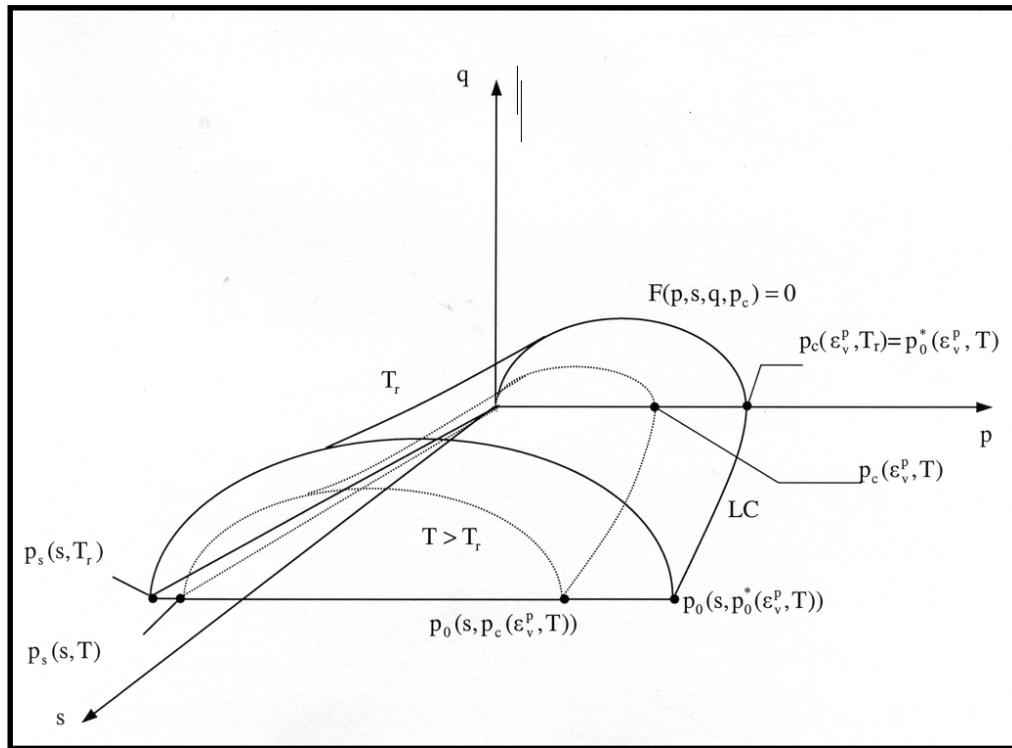


Fig. 4: Yield Surface of the Thermoelastoplastic model

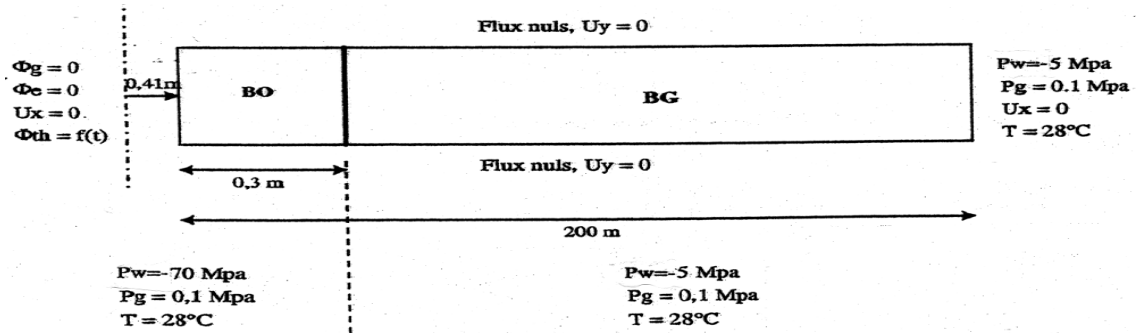


Fig. 5: Schematic model with the Boundary conditions

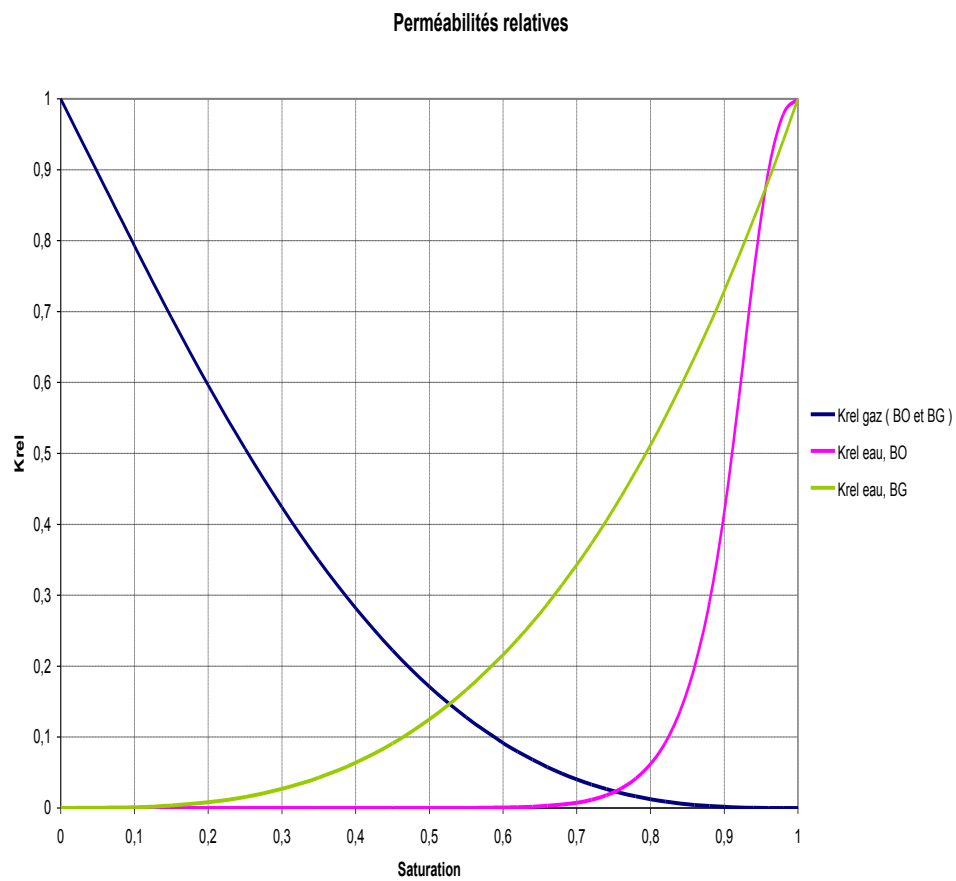


Fig. 6: Relative permeability of GB and of EB



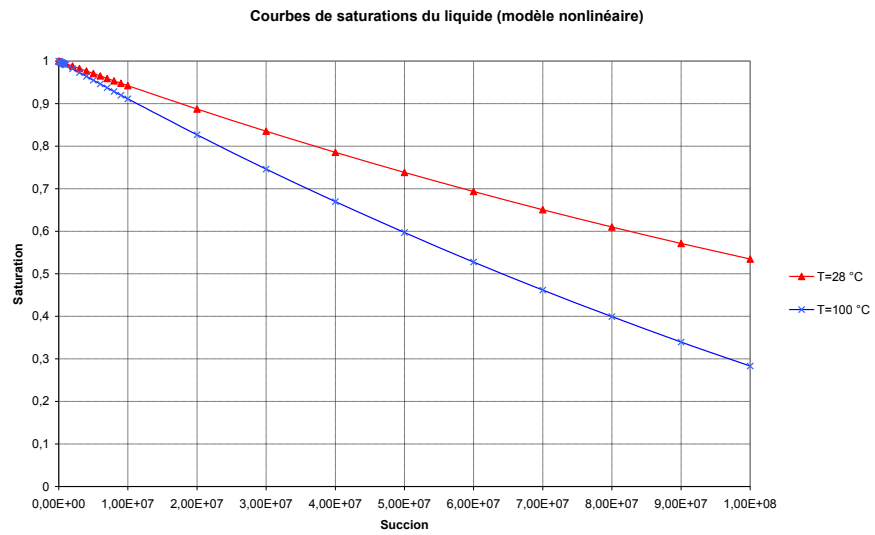


Fig. 7: State surface of degree of saturation

# Radial Displacement ; Nonlinear Model

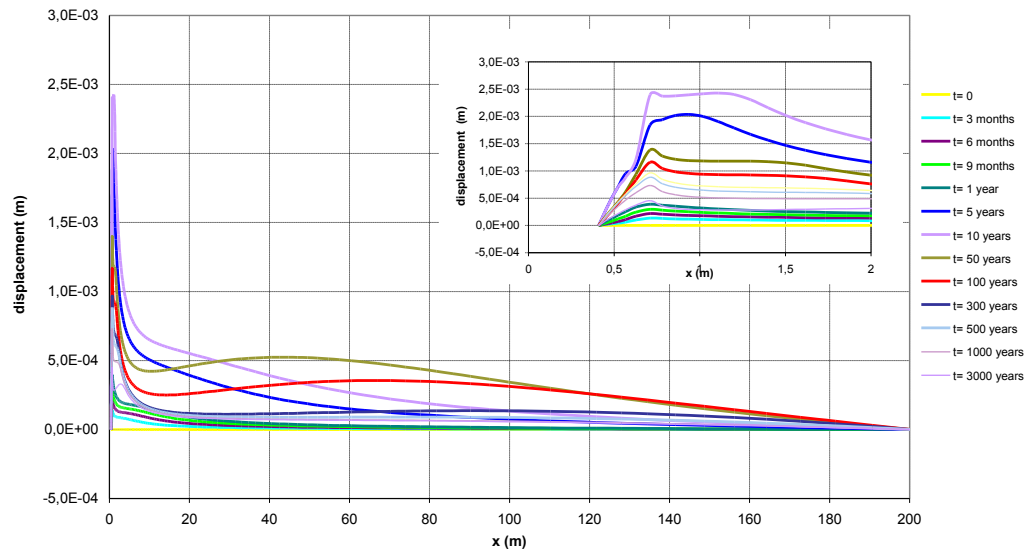


Fig. 8: Radial displacement variation in the medium

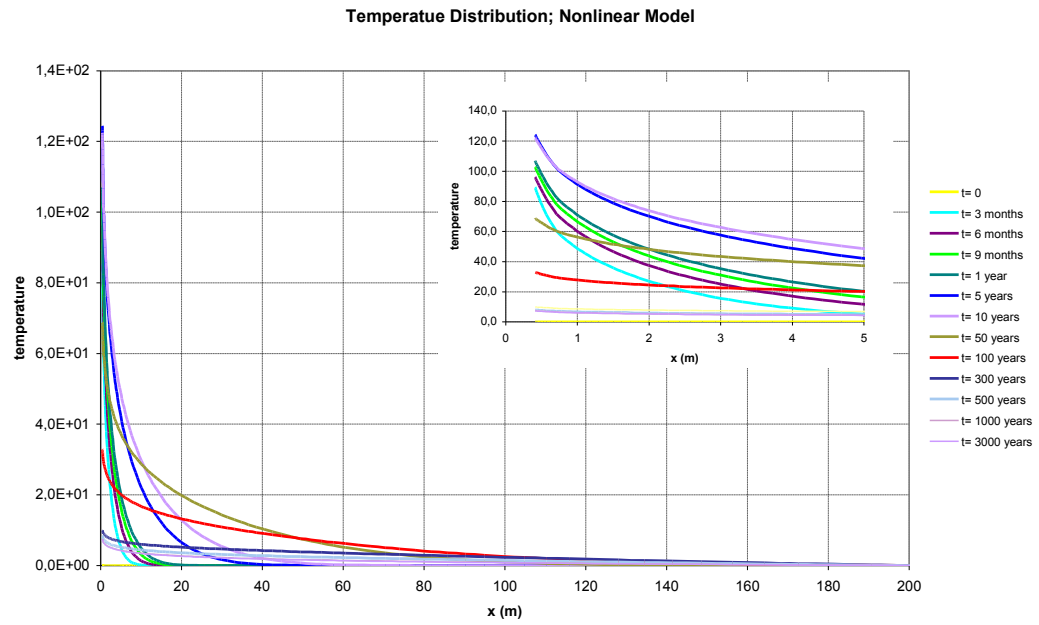


Fig. 9 : Temperature distribution in the massif

# Water Pore Pressure; Nonlinear Model

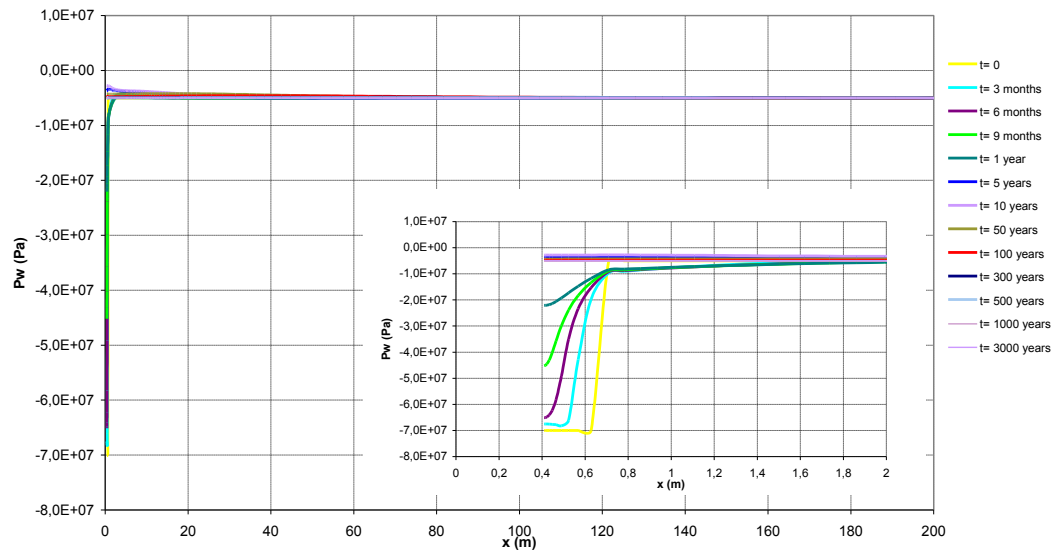


Fig. 10 : Water pore pressure distribution in the massif

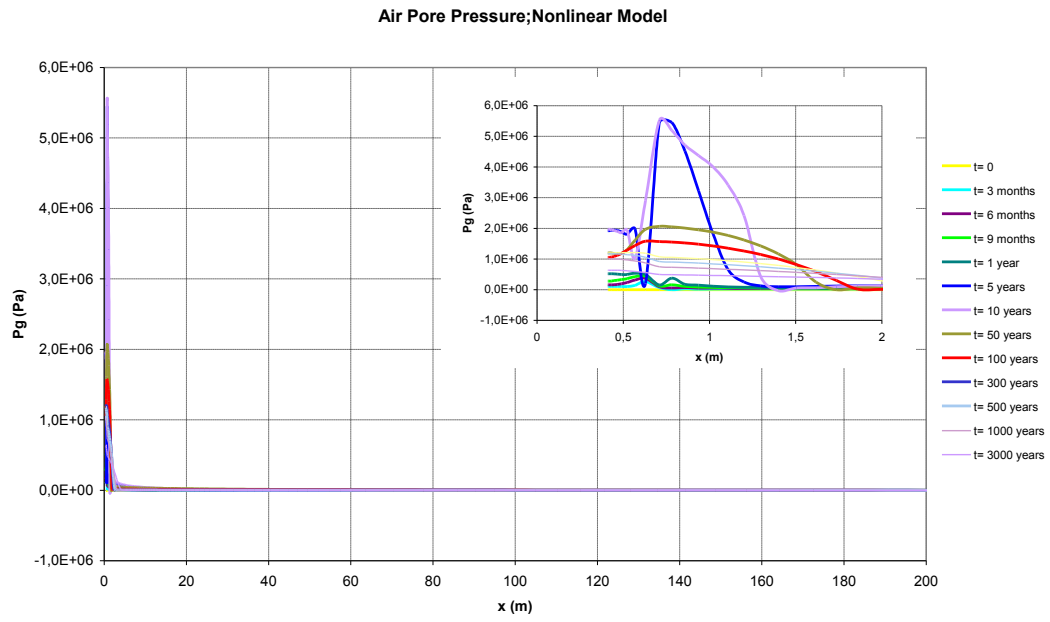


Fig. 11 : Air pore pressure distribution in the massif

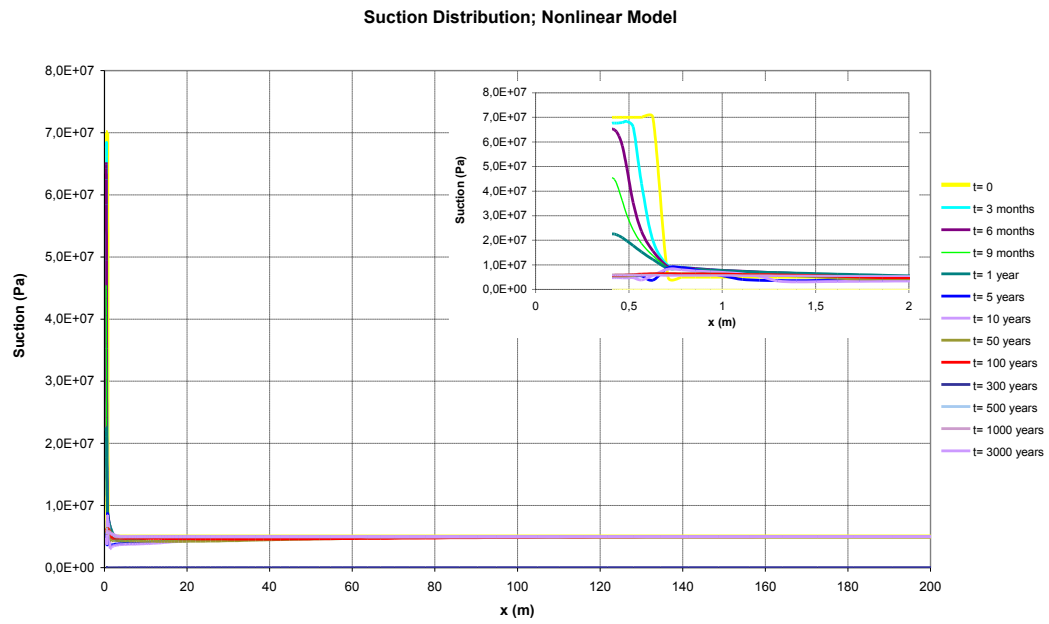


Fig. 12 : Suction variation in the engineered and geological barriers

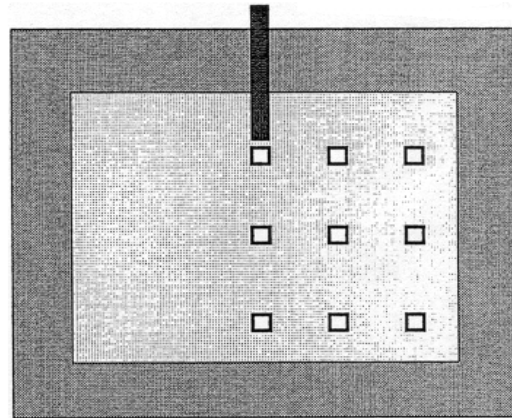
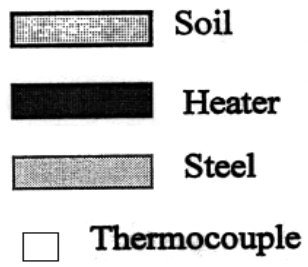


Fig. 13 : Configuration of experimental cell

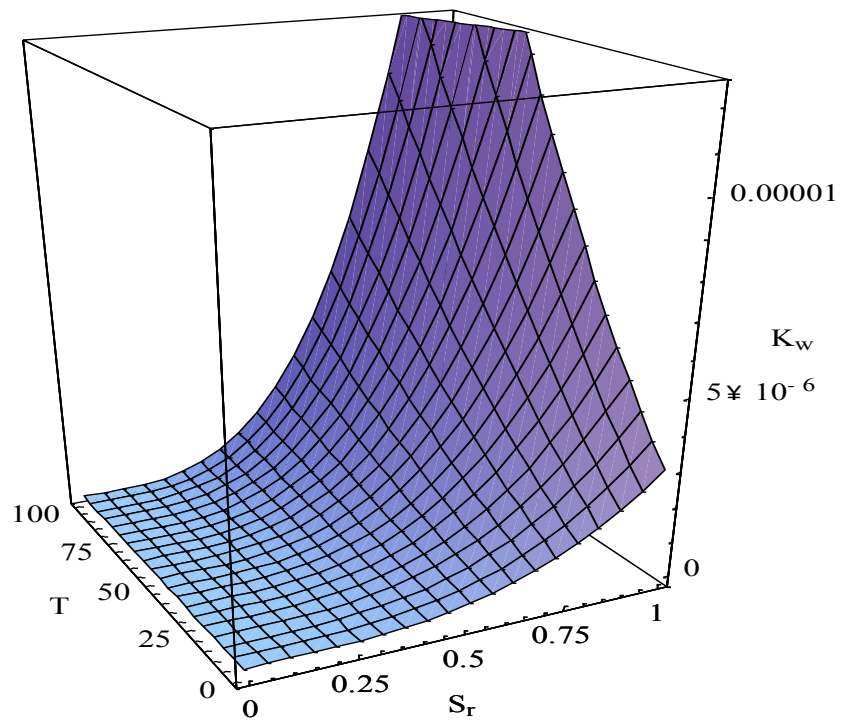


Fig. 14: Water permeability (in m/s) variation with temperature and degree of saturation.



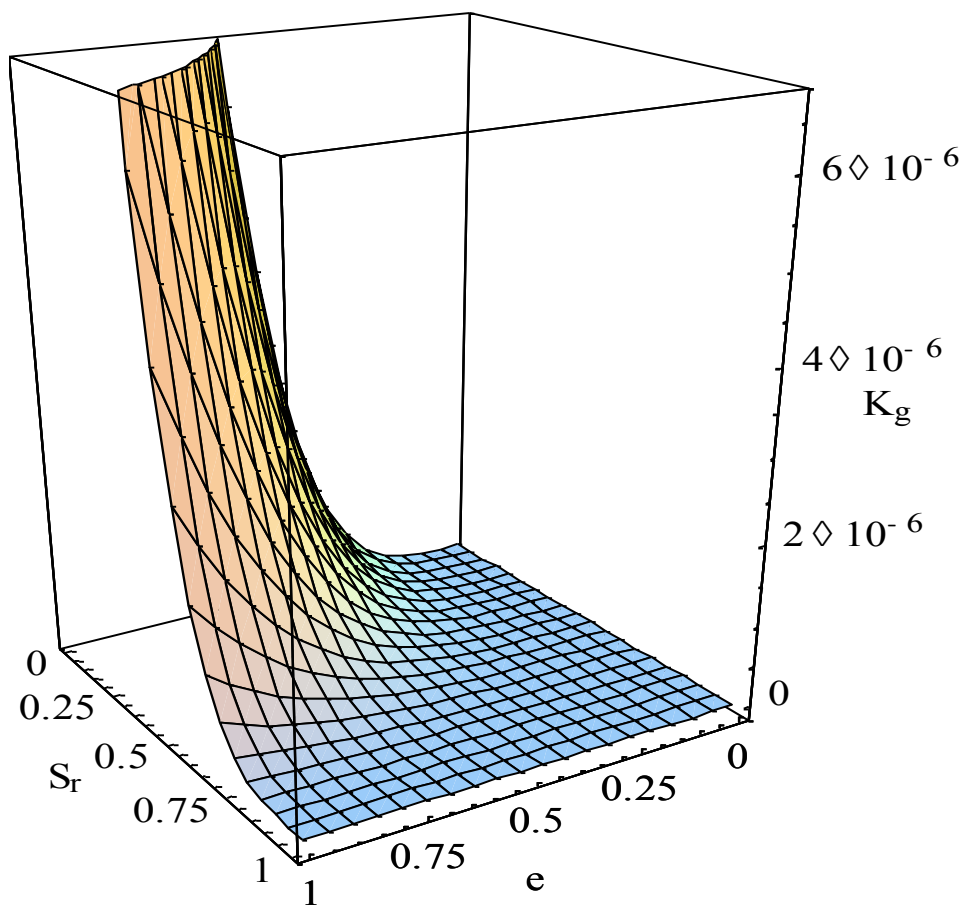


Fig. 15: Air permeability (in m/s) variation with temperature and degree of saturation

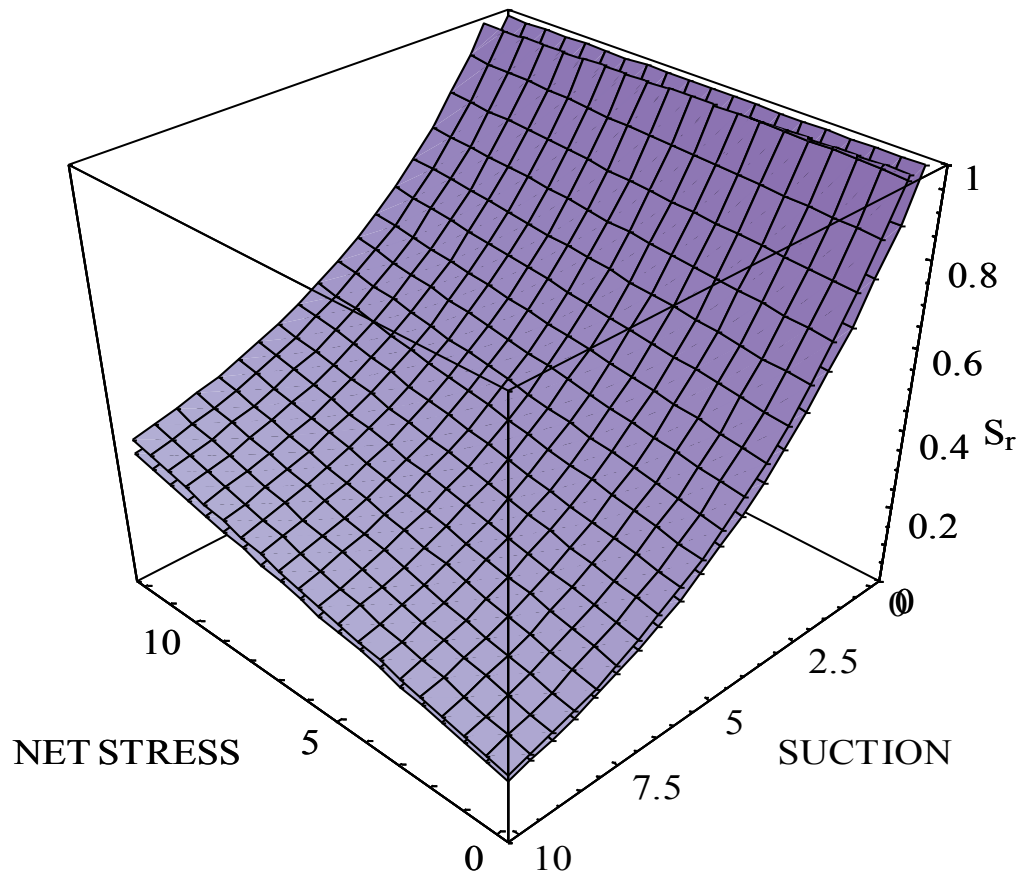


Fig. 16: State surface of void ratio for two different temperature as functions of suction and net stress

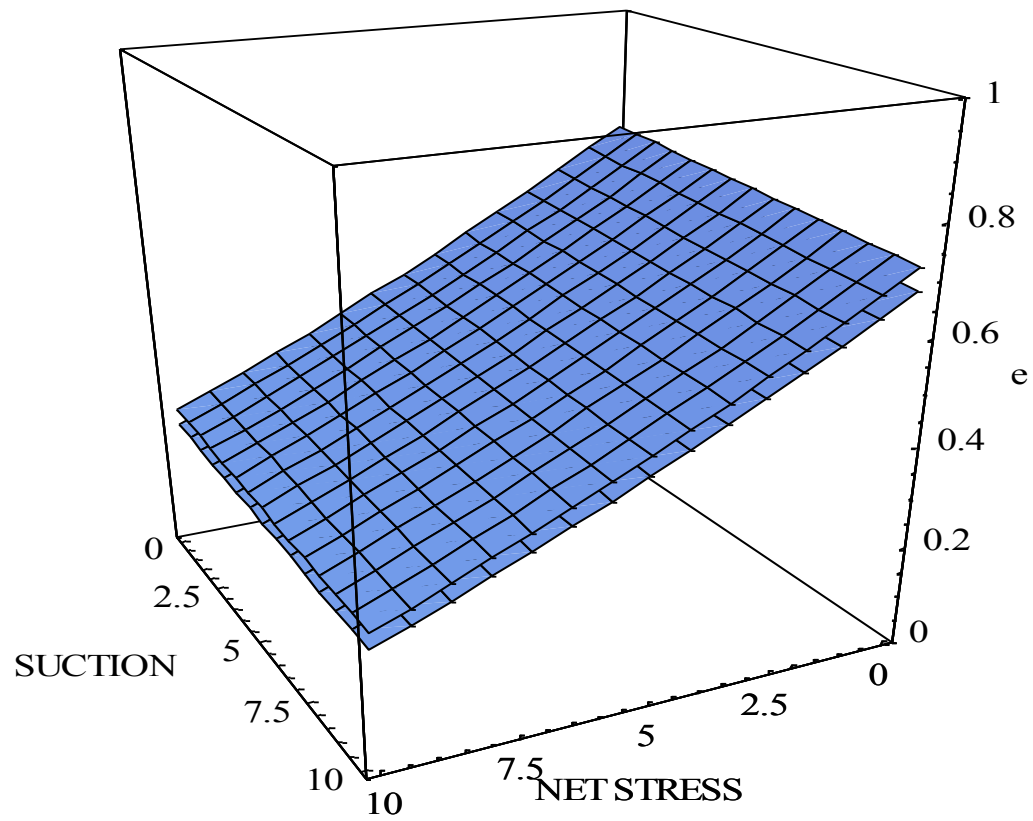


Fig. 17: State surface of degree of saturation for two different temperature as functions of suction and stress

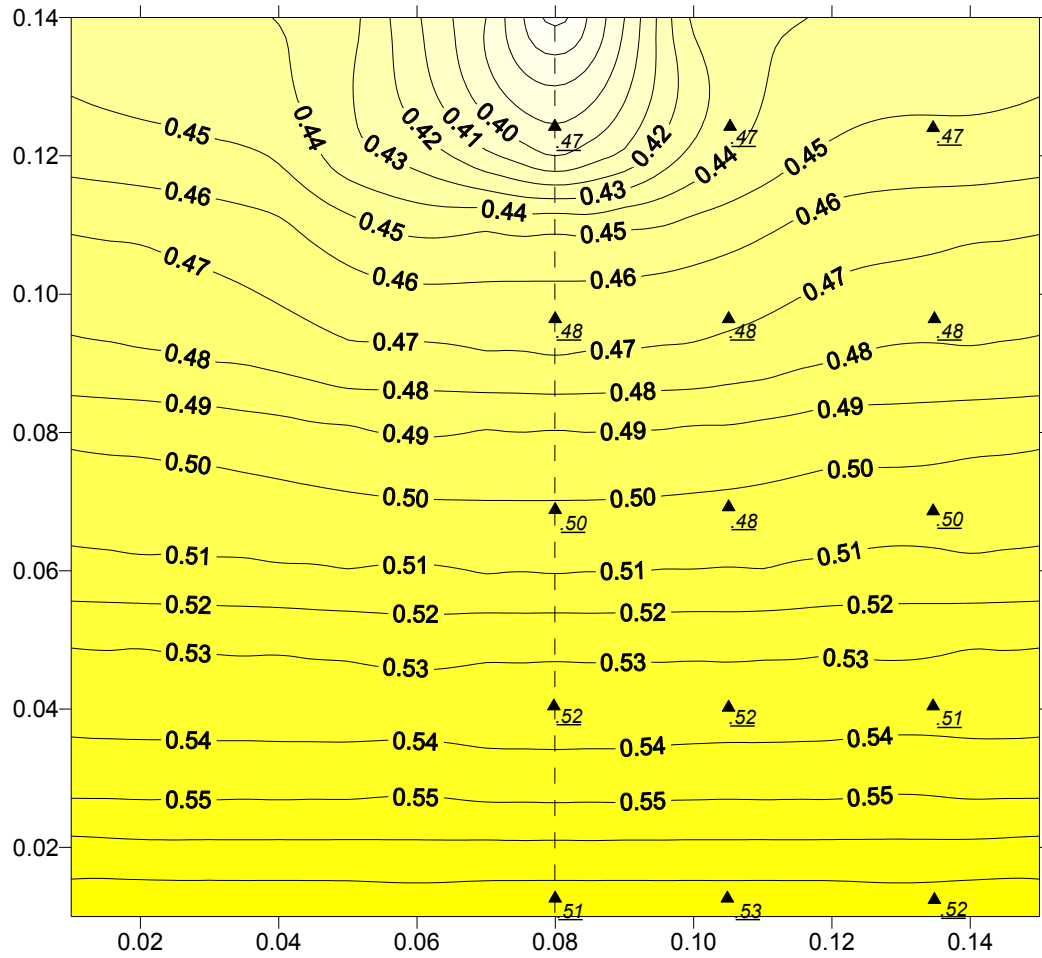


Fig. 18 : Degree of saturation values at the end of test (t=2 hours) - points are experimental values.

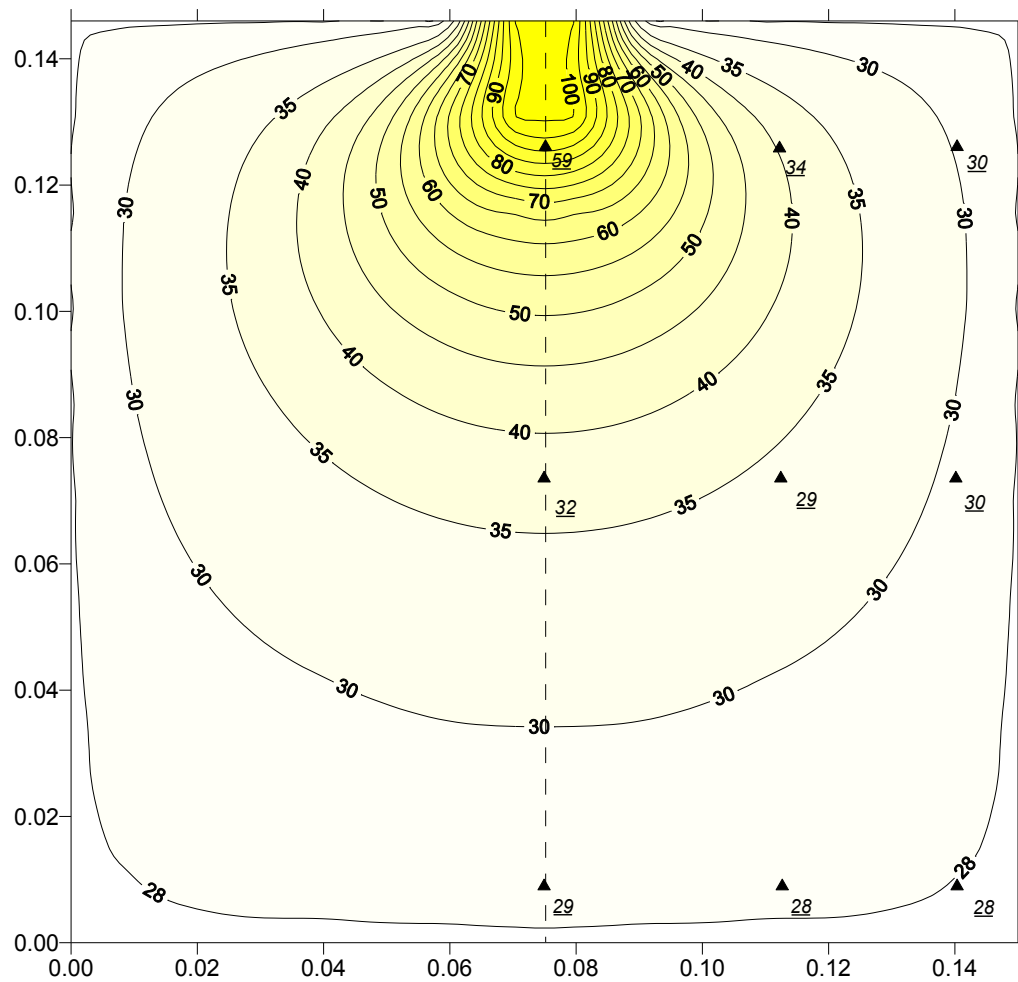


Fig. 19 : Temperature values the end of test ( $t=2$  hours) - points are experimental values.

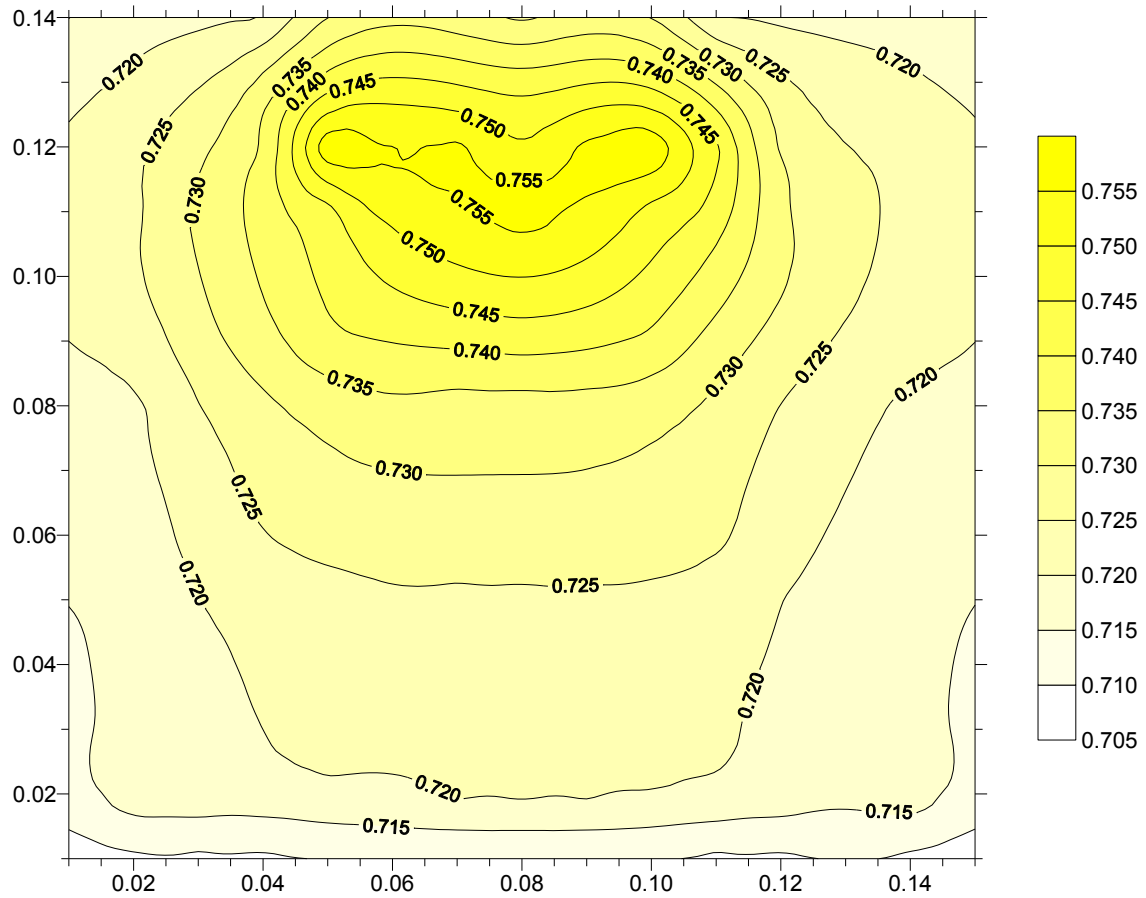


Fig. 20 : Void ratio values at the end of test

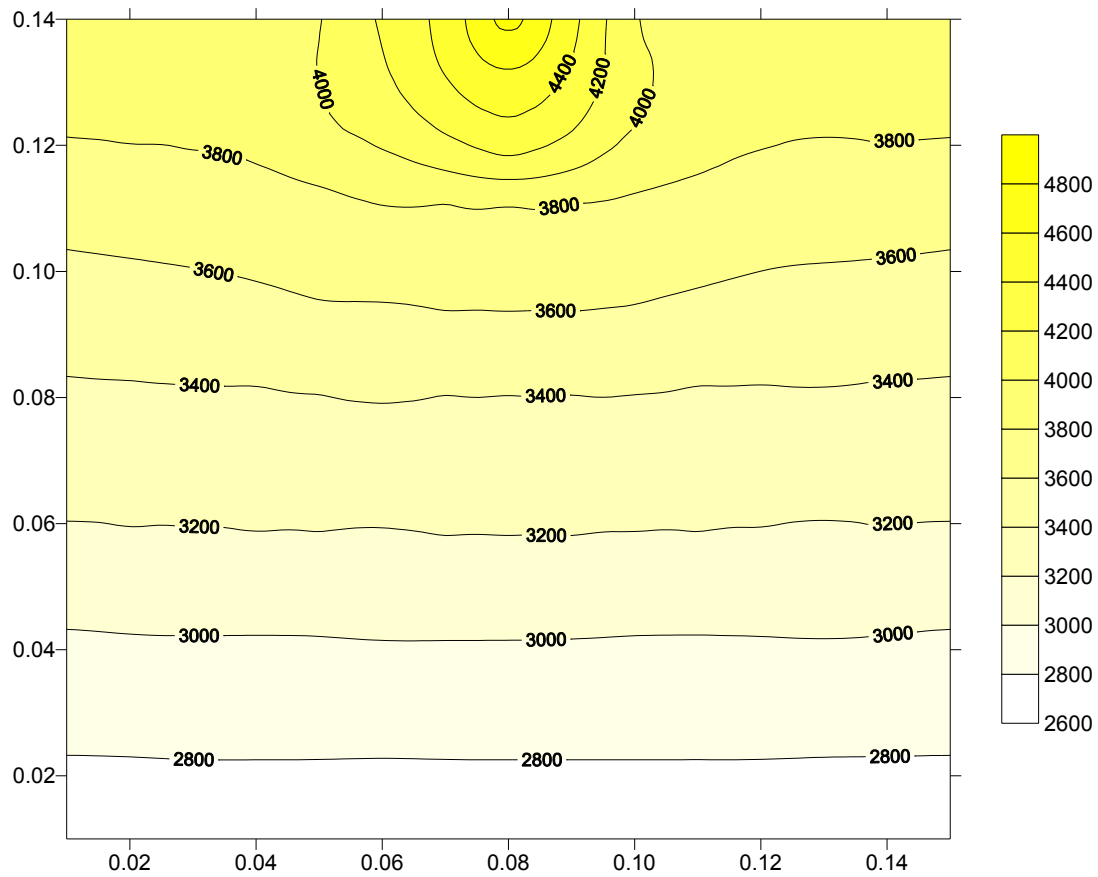


Fig. 21 : Suction values the end of test

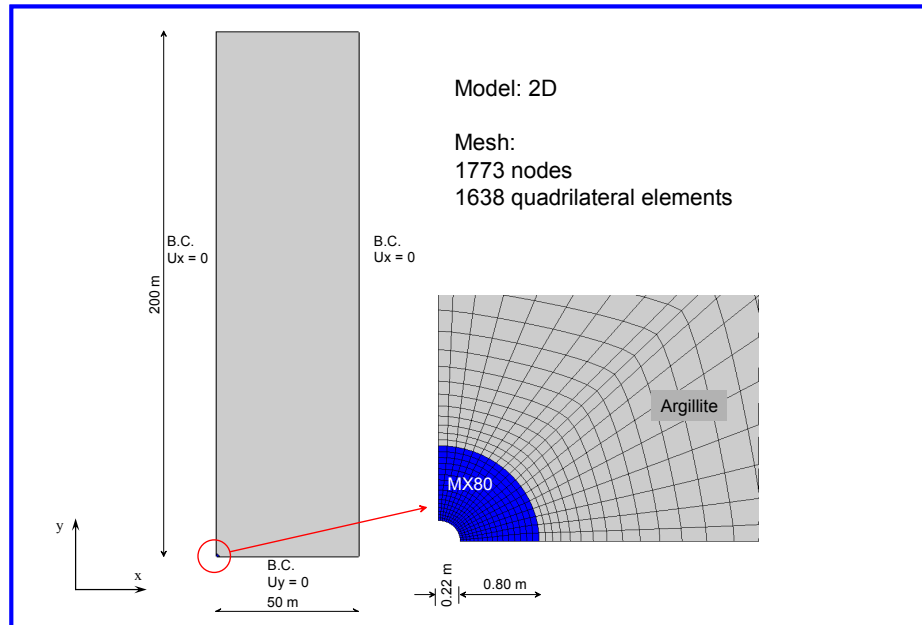


Fig. 22 : Geometry, mesh and boundary conditions of two dimensional elastoplastic model



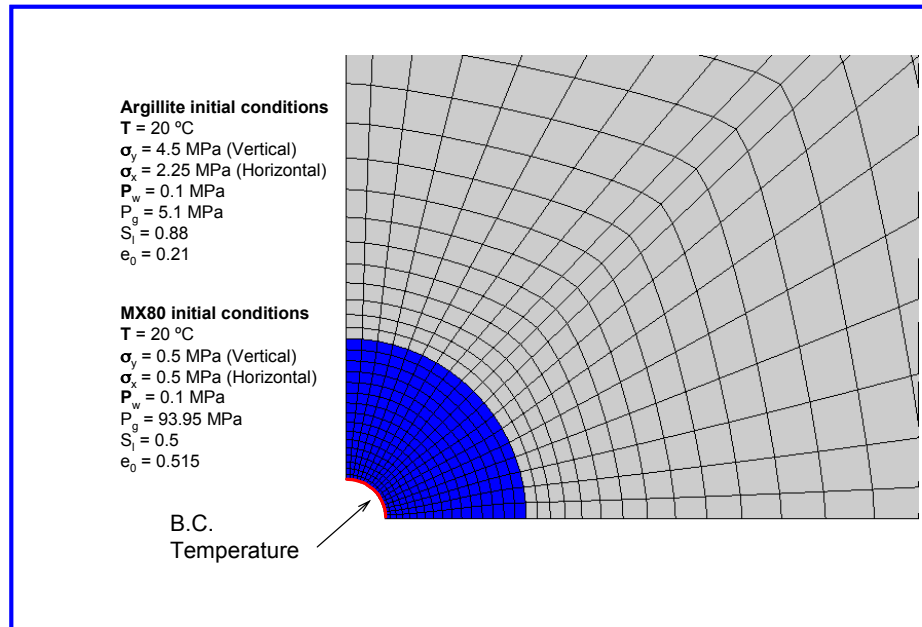


Fig. 23 : The initial conditions of Argilite and MX80

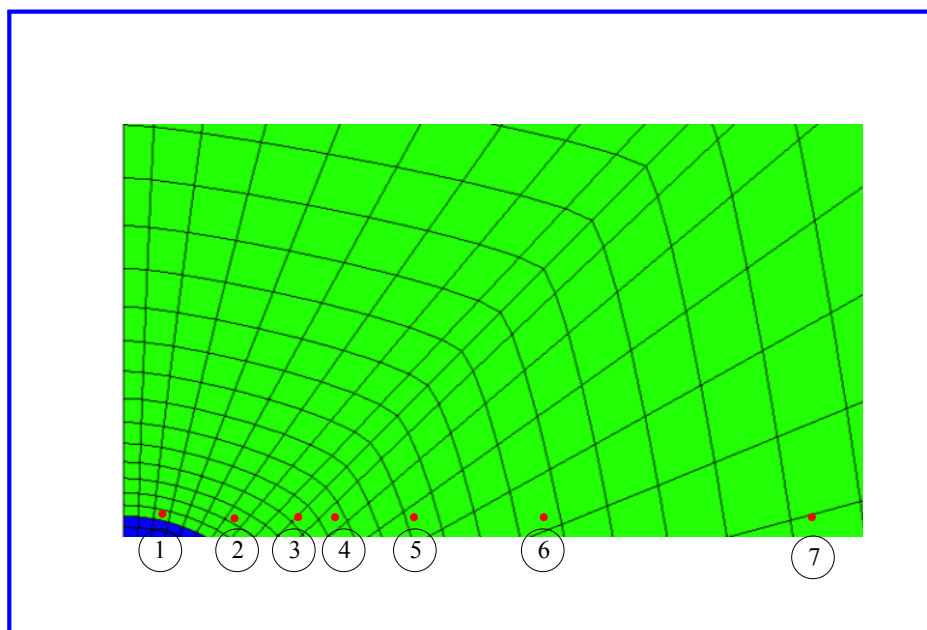


Fig. 24 : The points for which the results are presented

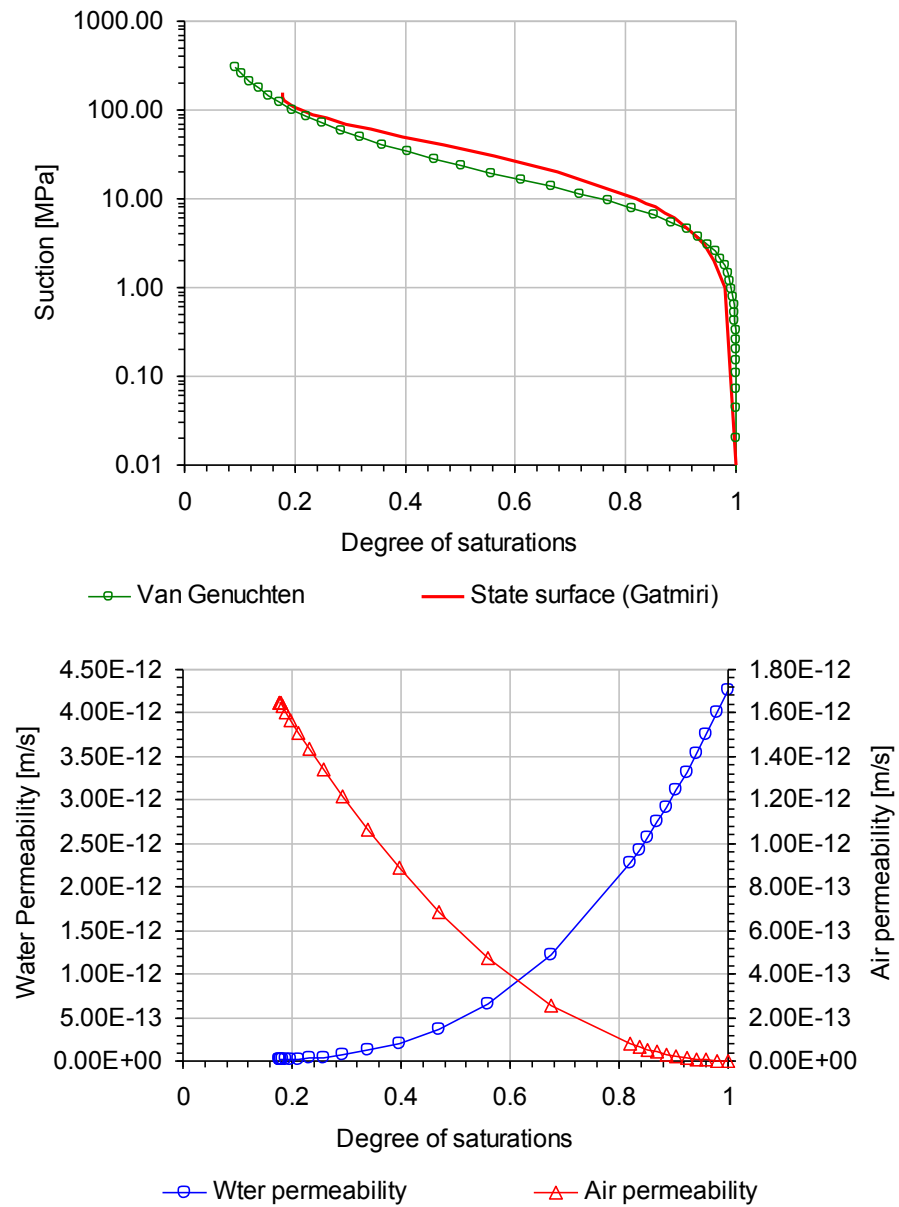


Fig. 25 : a) Comparison of state surface of saturation and water retention curve of Argilite  
b) Variation of water and air permeability with the degree of saturation of Argilite

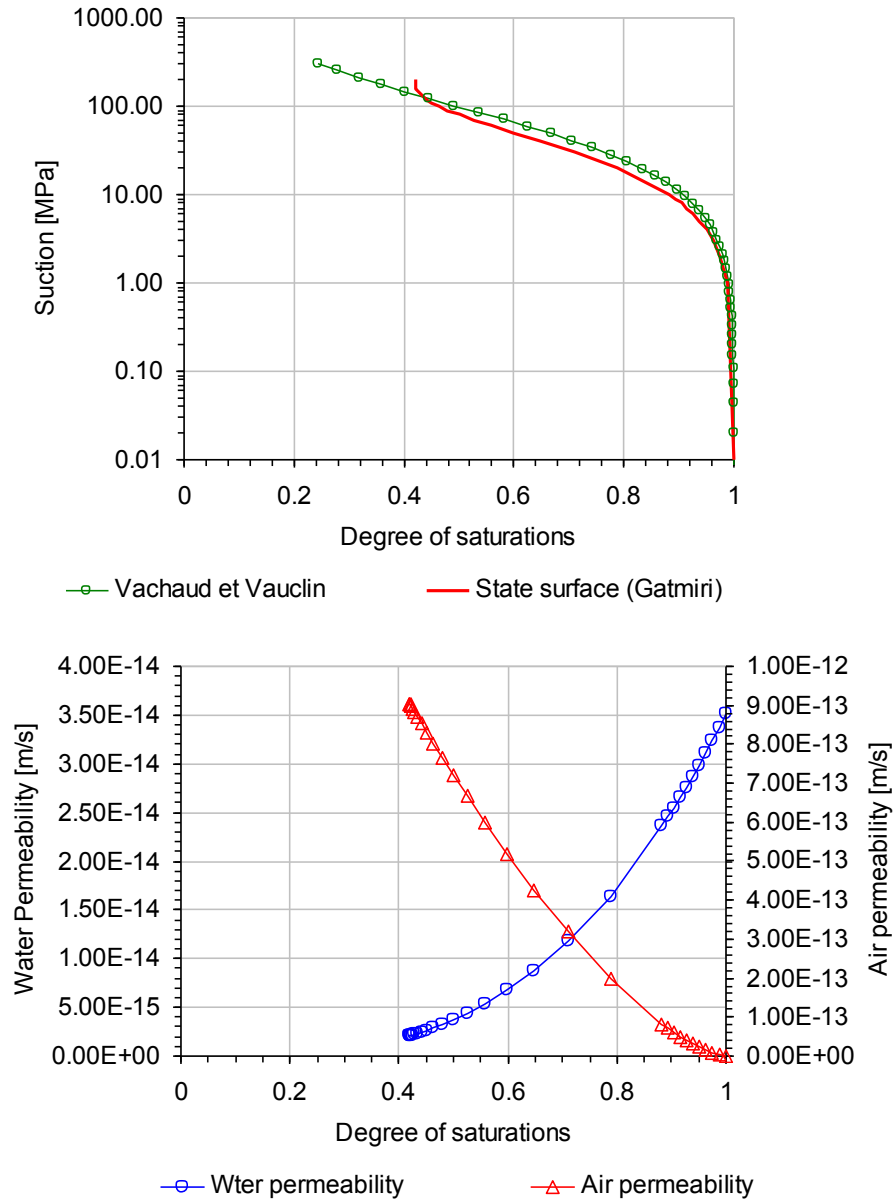


Fig. 26 : a) Comparison of state surface of saturation and water retention curve of MX80  
b) Variation of water and air permeability with the degree of saturation of MX80

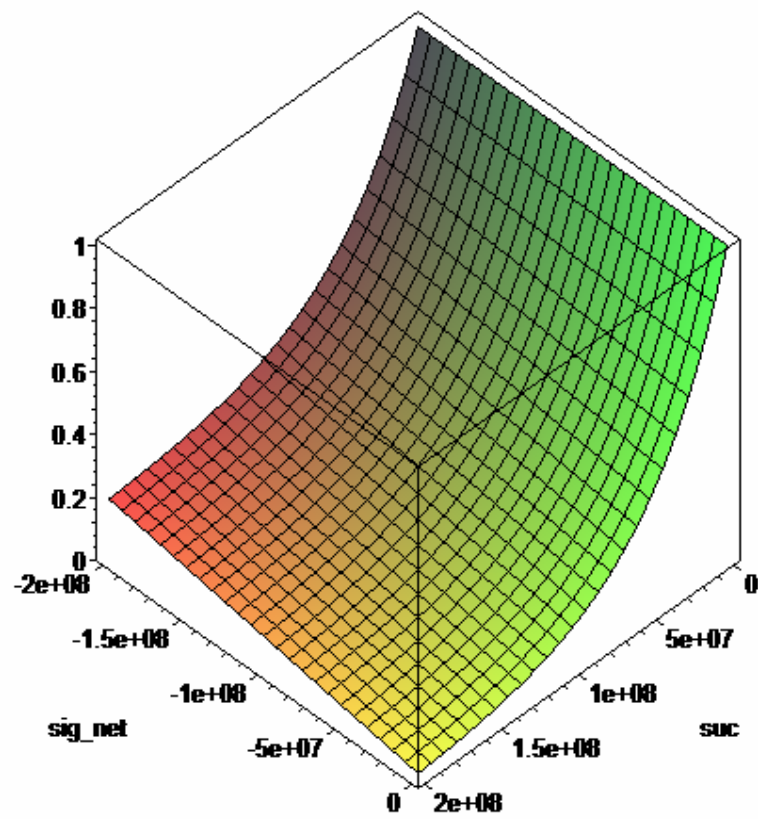


Fig.27 : Schematic presentation of state surface of degree of saturation of Argilite

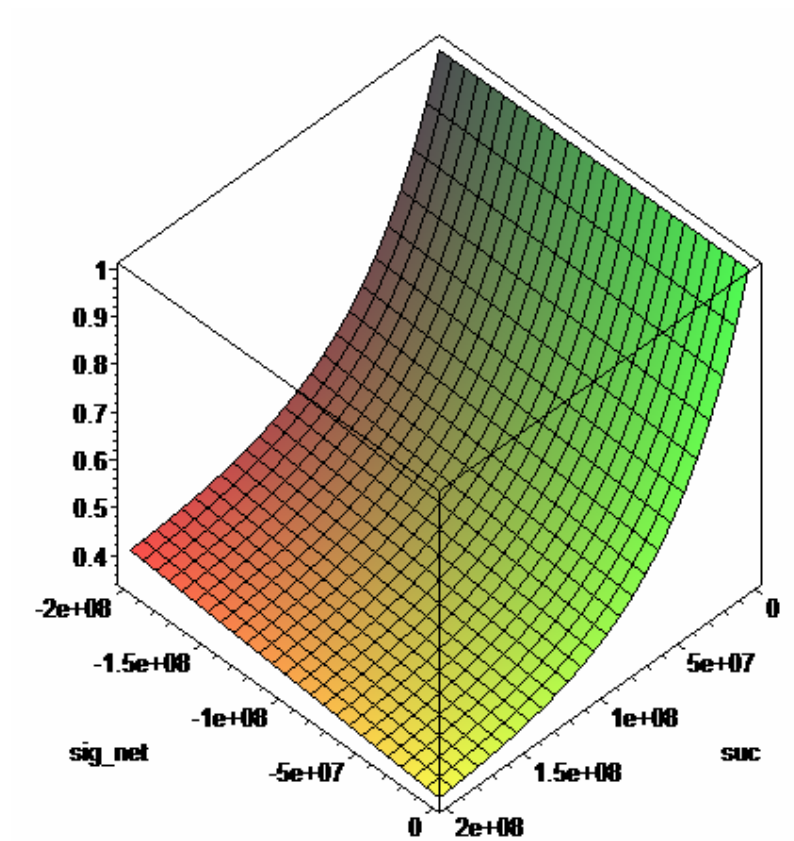


Fig.28 : Schematic presentation of state surface of degree of saturation of MX80

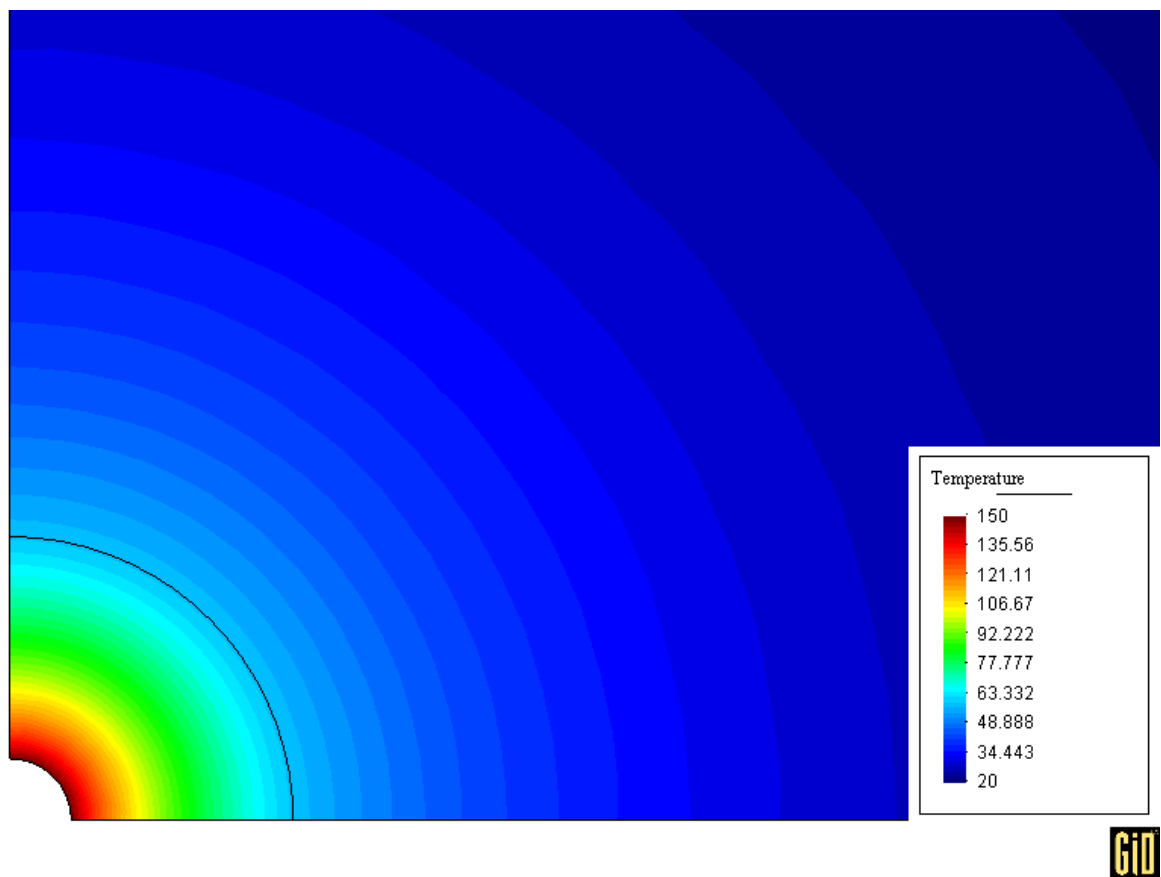


Fig. 29 : Temperature distribution with a THM elastoplastic model

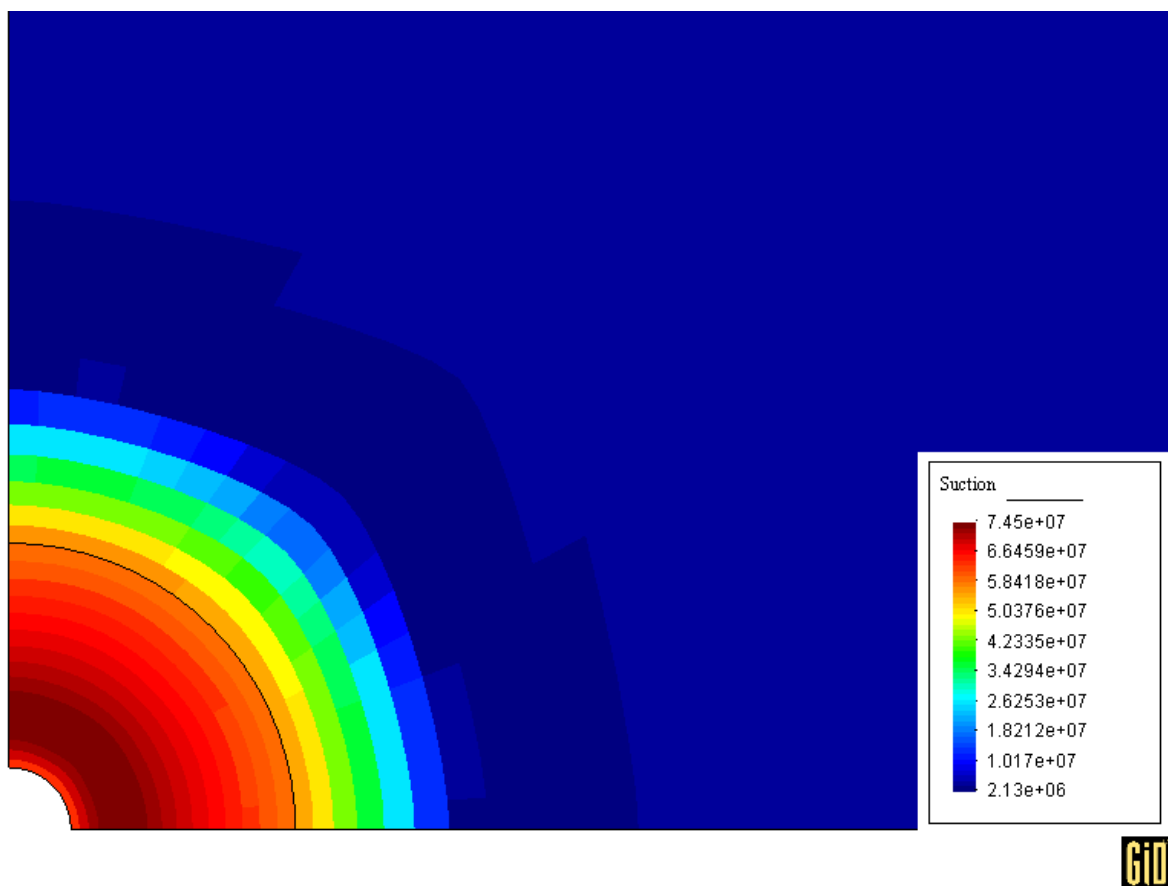


Fig. 30 : Suction distribution with a THM elastoplastic model



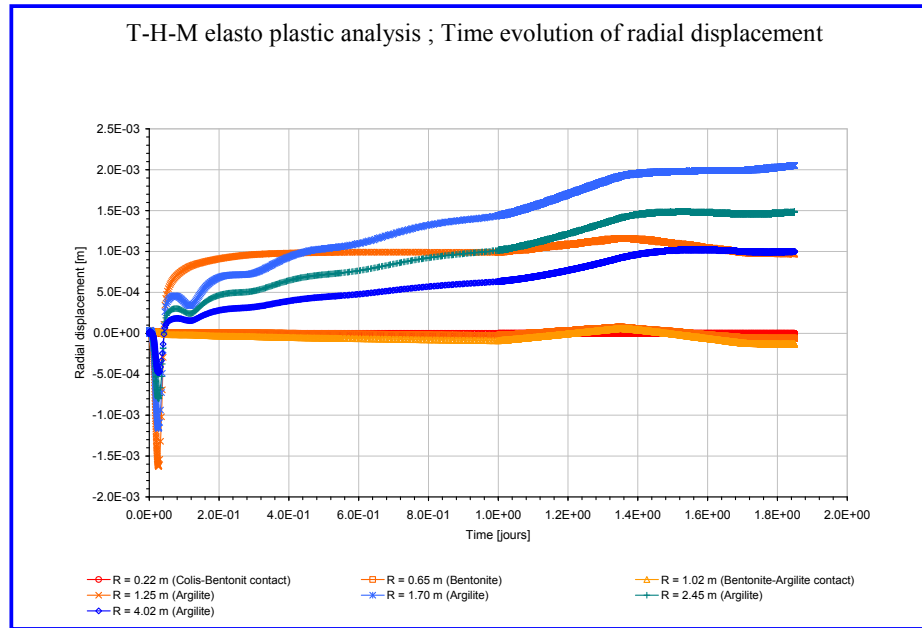


Fig.31 : Time evolution of radial displacement in elastoplastic modeling

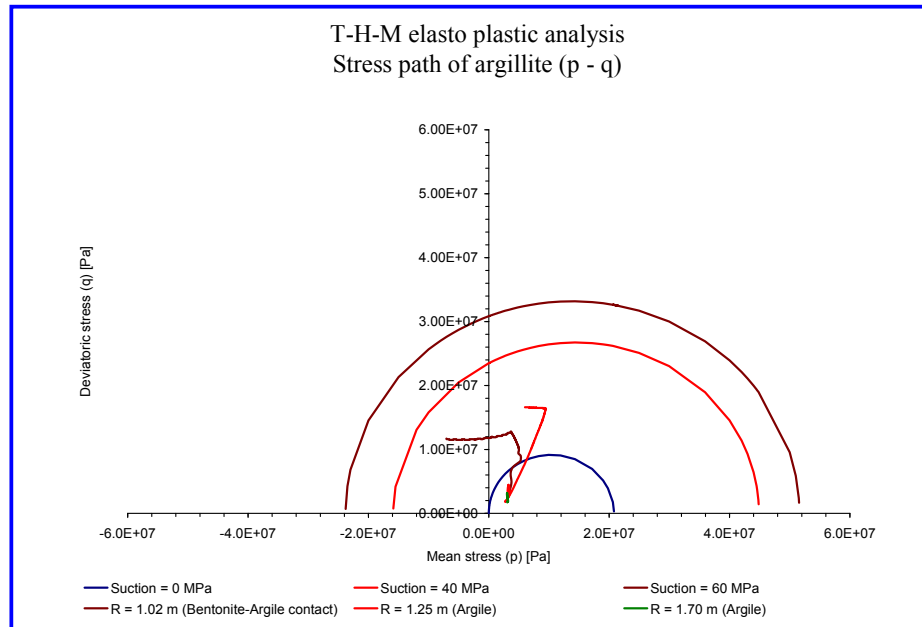


Fig. 32 : Stress path and yield surface of Argilite

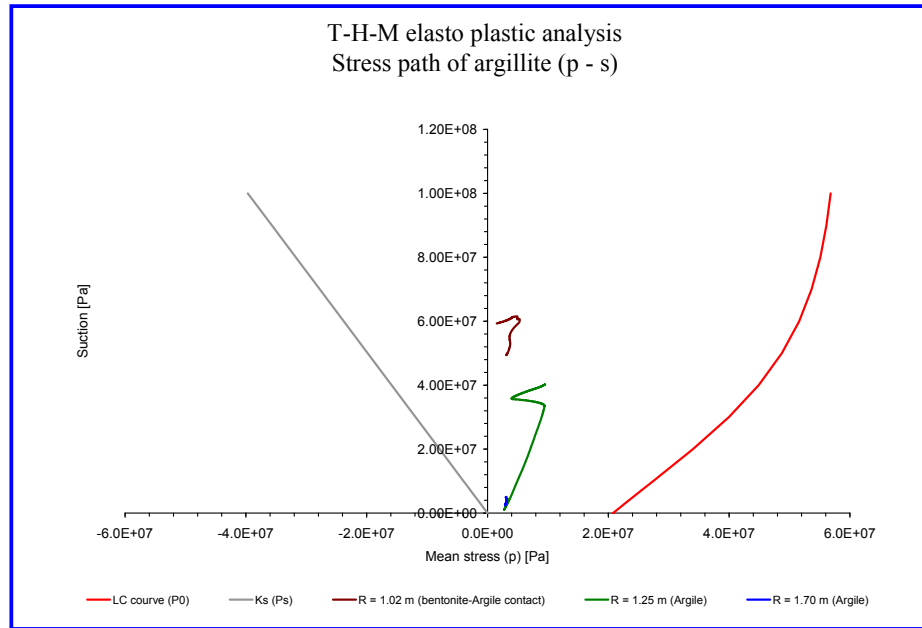


Fig. 33 : Stress path and LC of Argilite in P-S coordinates

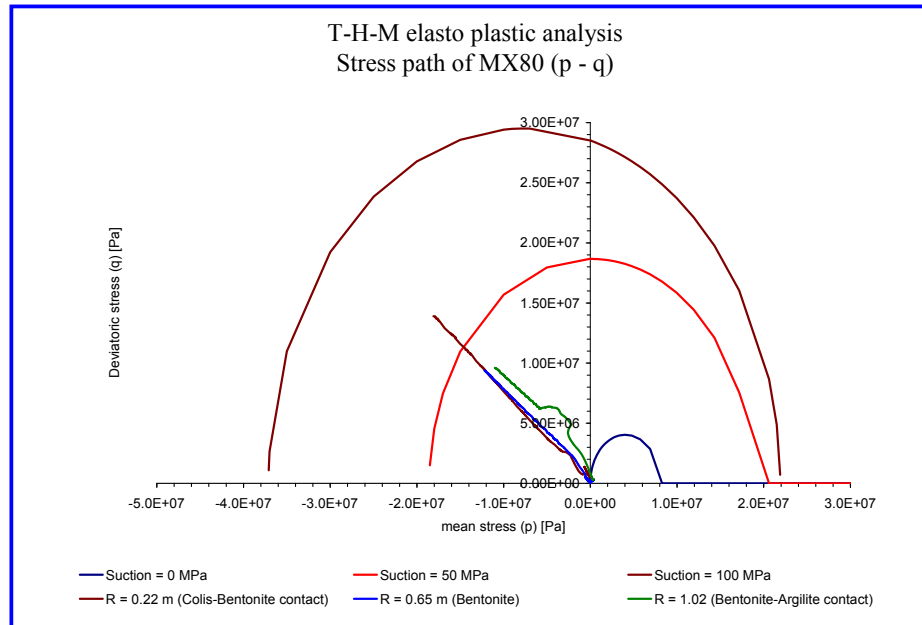


Fig. 34 : Stress path and yield surface of MX80

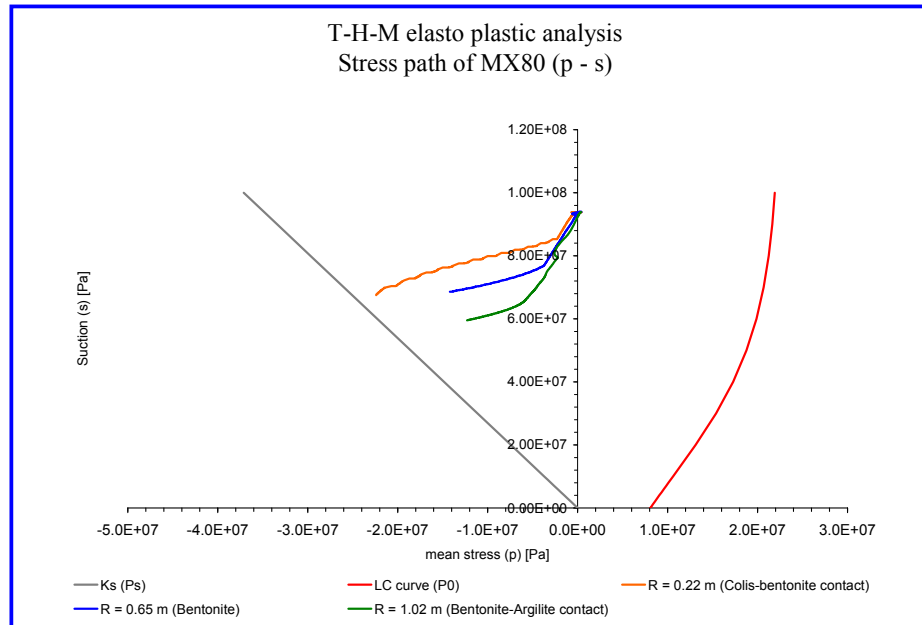


Fig. 35 : Stress path and LC of MX80 in P-S coordinates

Instant (sec)	Thermal flow
0.	149,8
31536.E4	121,1
63072.E4	95,1
94608.E4	78,8
126144.E4	66
157680.E4	51,4
220752.E4	33,6
283824.E4	23,9
378432.E4	15,7
473040.E4	10,95
630720.E4	7,88
946080.E4	4,89

Table 1: Temperature flow in time

Parameter	EB	GB
$K_l$	399	1678
$K_u$	399	1678
$K_b$	519	3281
$l/K_s$	7,1 E -10	7,1 E -10
$R_f$	0,75	0,75
$n$	0,6	0,6
$m$	0,4	0,4
$m \ 1$	0	0
$m \ 2$	0	0
$\rho_s$	2670 Kg/m <sup>3</sup>	2670 Kg/m <sup>3</sup>
$\rho$	2200 Kg/m <sup>3</sup>	2410 Kg/m <sup>3</sup>
$\nu$	0,2	0,3

Table 2: Mechanical parameters

Hydraulic Parameters		
Parameter	EB	GB
$l/K_w$	5,0E-10	5,0E-10
$K_{int}$	1,0E-20	1,0E-19
$\mu_g$	1,8E-5	1,8E-5
$\mu_w$	1,0E-3	1,0E-3
$\rho_w$	1000,0	1000,0

Table 3: Hydraulic parameters



Thermal Parameters		
Parameter	EB	GB
$h_{fg}$	2,4E6 J/Kg	2,4E6 J/Kg
$\lambda_a$	0,0258 J/m/s/°C	0,0258 J/m/s/°C
$\lambda_s$	1,77 J/m/s/°C	2,0 J/m/s/°C
$\lambda_w$	0,6 J/m/s/°C	0,6 J/m/s/°C
$C_p^s$	659,0 J/Kg/°C	575,0 J/Kg/°C
$C_p^w$	4180,0 J/Kg/°C	4180,0 J/Kg/°C
$C_p^v$	1870,0 J/Kg/°C	1870,0 J/Kg/°C
$C_p^a$	1000,0 J/Kg/°C	1000,0 J/Kg/°C
$\alpha_s$	2,0E-5/°C	2,0E-5/°C
$\alpha_w$	1,0E-4/°C	1,0E-4/°C

Table 4: Thermal parameters

<b>Notation</b>	<b>Argilite</b>
<b>M</b>	<b>0,88</b>
<b>K<sub>s</sub></b>	<b>0,008</b>
<b><math>\alpha</math></b>	<b>0,2e-2</b>
<b><math>\lambda_0</math></b>	<b>0,028</b>
<b>r</b>	<b>0,06</b>
<b><math>\beta</math></b>	<b>0,0076</b>
<b><math>\alpha_1</math></b>	<b>0,45e-5</b>
<b><math>\alpha_2</math></b>	<b>0,36e-6</b>
<b><math>\kappa_i</math></b>	<b>0,005</b>
<b>e<sub>0</sub></b>	<b>0,14</b>
<b>P<sub>c0</sub></b>	<b>20 MPa</b>
<b>a<sub>1</sub></b>	<b>-0,9 e4</b>
<b>a<sub>2</sub></b>	<b>-0,47e2</b>
<b><math>\alpha_0</math></b>	<b>2e-5</b>
<b><math>\alpha_3</math></b>	<b>0,24e-7</b>
<b>C</b>	<b>2 -3 MPa</b>

Table 5 : Parameters of Elastoplastic model for Argilite

Notation	MX80
$e$	0,515
$T_0$	20 °C
$s_0$	110 MPa
$p_{ini}$	0,1 MPa
$\kappa$	0,005
$\kappa_s$	0,001
$\alpha_0$	0,004 °C <sup>-1</sup>
$p_c$	0,5 MPa
$p_0^*$	10 Mpa
$\lambda(0)$	0,08
$r$	0,9
$\beta$	1

Table 6 : Parameters used in analysis for MX80

	$\rho^S$ (g.cm-3)	$C^S$ (J.kg <sup>-1</sup> .K <sup>-1</sup> )	$\lambda^S$ (W.K <sup>-1</sup> .m <sup>-1</sup> )
MX-80	2.67	1050	1.15
Argilite	2.67	775.5	1.8

Table 7 : Material Parameters of Argilite and MX80

$\rho^L$ (g.cm-3)	$C^L$ (J.kg <sup>-1</sup> .K <sup>-1</sup> )	$\lambda^L$ (W.K <sup>-1</sup> .m <sup>-1</sup> )	$\alpha^L$ (K <sup>-1</sup> )
1	4180	0.6	10 <sup>-4</sup>

Table 8 : Liquide Phase properties